



HAL
open science

Origin and fate of the greatest accumulation of silver in ancient history

Janne Blichert-Toft, François de Callataÿ, Philippe Télouk, Francis Albarède

► To cite this version:

Janne Blichert-Toft, François de Callataÿ, Philippe Télouk, Francis Albarède. Origin and fate of the greatest accumulation of silver in ancient history. *Archaeological and Anthropological Sciences*, 2022, 14 (4), pp.64. 10.1007/s12520-022-01537-y . hal-03616329

HAL Id: hal-03616329

<https://hal.science/hal-03616329v1>

Submitted on 22 Mar 2022

HAL is a multi-disciplinary open access archive for the deposit and dissemination of scientific research documents, whether they are published or not. The documents may come from teaching and research institutions in France or abroad, or from public or private research centers.

L'archive ouverte pluridisciplinaire **HAL**, est destinée au dépôt et à la diffusion de documents scientifiques de niveau recherche, publiés ou non, émanant des établissements d'enseignement et de recherche français ou étrangers, des laboratoires publics ou privés.

1 Origin and fate of the greatest accumulation of silver in ancient history

2
3
4 3 *Janne Blichert-Toft^{1*}, François de Callataÿ², Philippe Télouk¹, and Francis Albarède¹*

5
6 4 ¹ Laboratoire de Géologie de Lyon, CNRS UMR 5276, Ecole Normale Supérieure de Lyon, and Université de
7
8 5 Lyon, 46 Allée d'Italie, 69007, Lyon, France

9
10 6 ² Royal Library of Belgium, Boulevard de l'Empereur 4, 1000 Bruxelles, Belgium

11
12 7
13
14 8 *Corresponding author: jblicher@ens-lyon.fr; +33(0)608134849

15
16 9
17 10
18
19 11 **Keywords:** Silver coins, Pb isotopes, Achaemenid treasures, Alexander the Great, Greece,
20
21 12 Persia, India, convex hull

23 13 24 14 **Abstract**

25 15 The capture of the Achaemenid treasuries in 331-330 BCE by Alexander the Great in
26
27 16 Persepolis and Susa marked the demise of the 300-year old Persian empire and the era of
28
29 17 Hellenistic kingdoms. Alexander seized the equivalent of about 5,000 tons of silver, which
30
31 18 represented the accumulated tributes paid by subjugated people from the Aegean Sea to the
32
33 19 Indus to their Achaemenid rulers. Die studies show that this gigantic amount of silver, the so-
34
35 20 called 'Persian mix', had been used to produce most of the coinage of Alexander the Great
36
37 21 himself and to an even greater extent those of the Diadochi, his successors. What remains to
38
39 22 be understood is the origin of the silver of this immense treasure. Lead isotope abundances
40
41 23 determined on both Persian *sigloi* and *alexanders* struck from Achaemenid silver trace the
42
43 24 bullion source to the southern Aegean, Macedonia, and Thrace. Lead in pseudo-coinage from
44
45 25 early Indian kingdoms is isotopically different from the rest, which attests to a limited Indian
46
47 26 contribution to the Achaemenid treasuries. Studies of Iron Age hoards from the Levant leave
48
49 27 open the possibility that the making of the Persian mix may have predated the Achaemenid
50
51 28 expansion of the 7th century BCE. We speculate on the motivations of such massive hoarding
52
53 29 by the Persian kings and on its economic implications.

54 30 55 31 **1. Introduction**

56 32 The 331 BCE defeat of the Persian Achaemenid king Darius at Gaugamela, next to modern
57
58 33 Erbil, Iraqi Kurdistan, opened the road to Susa, Babylon, and Persepolis to Alexander the
59
60
61
62
63
64
65

34 Great. The colossal amount of wealth plundered by the Macedonians, in particular from the
35 royal treasury in Persepolis, has been described by a number of ancient writers such as
36 Curtius, Diodorus, Plutarch, Arrian, and Justin (Callatay 1989; Holt 2016) and may have
37 reached up to 200,000 talents of Attic standard (1 talent = 25.9 kg), which in modern units
38 correspond to a staggering silver weight of about 5,200 metric tons. This estimate is an
39 aggregated value of gold and silver converted to Attic silver talents, for example 2,600 tons of
40 silver and 260 tons of gold. This figure has to be seen from the mercenary perspective: a
41 Greek hoplite received a daily stipend of about a drachm of 4.3 g. As such, 200,000 talents
42 represent 1,2 billion daily wages, enough to pay in fresh coins for an army of 50,000 soldiers
43 during more than 60 years.

44
45 Although heritage of silver accumulation by the Neo-Assyrian (911-605 BCE) and Neo-
46 Babylonian (626-539 BCE) empires in what would become the Persian Empire by looting,
47 trade, and tribute was certainly significant, the Achaemenid dynasty organized the captation
48 of silver resources on a regional scale very efficiently. As reported by Herodotus (III.95), the
49 yearly tribute was 14,560 talents. The looting of Persian treasuries by Macedonian armies
50 created one of the most massive releases of precious metals, superior to any other booty
51 known from Classical antiquity, such as the Egyptian treasury brought back to Rome by
52 Augustus (Nicolet 1984). How such a bullion deluge affected the various economies at the
53 time, and in particular commodity prices, has been the subject of much interest (Van der Spek
54 and van Leeuwen 2014), but, beyond the impact on commodity prices in Babylonia for less
55 than a generation (Jursa 2010), its effect on the Aegean market is not well documented.

56
57 What is known, however, is that, over three decades (ca. 332-301 BCE), most of the Persian
58 treasuries were converted into coins. Different forms of ‘money’ existed in Mesopotamia for
59 millennia, and among them barley and silver were the most prominent (Powell, 1996; Jura,
60 2014). The silver shekel, originally a measure of weight (8.3 g), had also gradually been
61 accepted as a unit of account and been used physically for trade, although far from
62 exclusively. Silver coinage was only briefly used in the Western part of the Empire for
63 military purposes (Alram 2012; Le Rider 2001). As pointed out by van der Spek et al. (2018),
64 the conquest by Alexander in 331 ushered in minted silver as the primary currency. The many
65 die studies conducted on the coinages of Alexander and his successors reveal that the full
66 production issued in gold and silver exceeded 100,000 talents (Callatay 1989; Callataj 1993;
67 Holt 2016; Meadows 2014). Moreover, coin metal analyses have shown that, for both gold

68 and silver, nearly all eastern production, as well as a substantial part of western production,
69 notably in Macedonia, are likely to have been issued from this bullion, hereafter referred to as
70 the ‘Persian mix’. Mixed bullion is consistent with both historical accounts attesting to a
71 Persian policy of remelting tribute and the homogeneous Au/Ag of silver Alexander issues
72 (Olivier et al. 2017).

73
74 Despite some modern discredit cast on Herodotus’ list of tributes to Darius (Armayer 1978;
75 Bresson 2020), this author famously testifies to the reality of the hefty tributes paid to the
76 King of Kings (the title used by Achaemenid Persian kings) by each satrapy (III.89-97). Most
77 revenues are expressed in silver talents but with some still paid in kind such as white horses
78 or frankincense, while it is also made clear that India paid in gold. Whether the actual tributes
79 were paid in silver, gold, horses, or frankincense cannot be known, but the massive minting of
80 silver coinage by Alexander and the Diadochi demonstrates that the Achaemenid palaces must
81 have been packed with vast amounts of bullion.

82
83 From where came the dormant silver heaps of the Persepolis and Susa vaults attested to by
84 ancient writers (Callatay 1989; Holt 2016)? The present work investigates the issue of the
85 origin of the Persian mix using high-precision lead isotope analysis in an attempt to
86 understand whether other silver ores, in addition to the well-acknowledged sources in the
87 Greek world, were involved in the treasures amassed by the King of Kings and what were the
88 particular motivations behind the hoarding of so much bullion.

89
90 In addition to Pb isotope measurements of silver Alexander coinage (*alexanders*), the present
91 work also presents data on two other types of silver coinage that were unlikely to have been
92 minted from the central Persian treasury. First, silver *sigloi* (shekel) are the only significant
93 coinage produced by the Persian empire in its western satrapies (Alram 1993; Tuplin 2014).
94 They are known, together with archaic Greek coins and Indian punch-mark coinage from
95 Gandhara, from the Kabul hoard deposited ca. 350 BCE (Schlumberger 1953), but so far have
96 not benefited from isotopic work (e.g., Kraay and Emeleus 1962). Second, although no
97 known evidence substantiates a significant input of Indian silver to Persian treasury
98 (Herodotus, III.98-105), the present work provides Pb isotope data on early Indian punch-
99 mark coinage to corroborate this conjecture by objective, concrete means (Reddy 2014).

100

2. Materials and Methods

The present work presents high-precision Pb isotope data on ancient silver coins produced in Persia during the Achaemenid reign and in the Hellenistic world in the immediate aftermath of Darius' defeat. The measured Pb isotope data were treated using novel statistical tools in the form of calculated Pb model ages combined with convex hull theory (see below), which allow the tracking of silver provenance with greater accuracy and precision than possible when using only raw Pb isotope ratios and manually comparing artefacts with known ores on a one-to-one basis. The coin types analyzed here are: (1) silver *alexanders*, minted both during the king's lifetime and shortly after his death; (2) silver *sigloi*; and (3) *shatamanas* (bent silver bars and imprinted pieces) from Gandhara and Kamboja janapadas (kingdoms), Northern India, generally dated from the 6th to the 4th century BCE, respectively. (4) A subset of Greek silver coins further was included for reference. The analytical techniques used for the determination of Pb isotope compositions have been described elsewhere (Milot et al. 2021) and involve anion-exchange chromatography for Pb separation and multi-collector inductively coupled plasma mass spectrometry (MC-ICP-MS) for Pb isotopic analysis. Here it suffices to state that all coins of (1), (2), and (3) were drilled, whereas coins of (4) were leached (37) (cf. Milot et al. 2021). Repeated measurements of NIST 981 throughout each analytical session consistently yielded an external reproducibility of <100 ppm (0.01%) for ²⁰⁴Pb-normalized ratios and <50 ppm (0.005%) for ²⁰⁷Pb/²⁰⁶Pb and ²⁰⁸Pb/²⁰⁶Pb. In-run errors systematically were smaller than the external reproducibility for all samples. [Table S1](#) (*Supplementary Information*) compiles relevant coin information with the corresponding Pb isotope data acquired in this study.

3. Lead isotopes and the convex hull strategy

The prevalent method of assessing provenance of silver artefacts is by means of Pb isotopes. Contrary to the abundances of stable isotopes of other elements, such as Cu and Ag, which vary with environmental conditions, the relative abundances of Pb isotopes vary predominantly as a result of uranium and thorium radioactive decay and consequent lead radiogenic ingrowth. Isotopic variations are controlled by the U/Pb and Th/Pb ratios of the rock from which the Pb ore was born and by the time elapsed up to that point. Time (Pb model age), U/Pb, and Th/Pb can be calculated from measured Pb isotopic compositions and be used to deduce the tectonic context in which the ore appeared. In practice, however, archeologists and numismatists simply manually compare the measured Pb isotopic compositions of artefacts in pairs of 2-dimensional plots, such as ²⁰⁸Pb/²⁰⁶Pb vs ²⁰⁷Pb/²⁰⁶Pb

135 and $^{204}\text{Pb}/^{206}\text{Pb}$ vs $^{207}\text{Pb}/^{206}\text{Pb}$, with those of ores stored in a database until they find a match
136 that is acceptable. However, it takes more than a match in one pair of diagrams to establish
137 whether a data point falls into the 3-dimensional field of Pb isotopic ratios of a particular
138 mining district (Fig. 1a). The Pb isotopic data must be visualized in 3-dimensional space (as
139 dictated by the number of parent isotopes, ^{238}U , ^{235}U , and ^{232}Th): although the projections of
140 two different points may coincide on the x-y and x-z planes, they can be distinct on the y-z
141 plane. Prior attempts to address this issue (Delile et al. 2014; Westner et al. 2020) have
142 demonstrated the multiple difficulties of assessing meaningful distances between points. Here
143 we therefore take a different approach, that of the so-called ‘convex hull’ (Fig. 1b), which was
144 previously proposed under the name of ‘isotopic niche’ in Ecology (Eckrich et al. 2020)
145 before it found its way into Archeology in general (Robinson 2021) and the provenancing of
146 Iron Age *hacksilber* from the Levant in particular (Gentelli et al. 2021).

147
148 The Pb isotope data on the different groups of coins, e.g. *sigloi*, are enclosed in the minimal
149 (circumscribing) 3-dimensional (3D) volume (Fig. 1c), the convex hull, which was expanded
150 by 5% to take into account potential analytical uncertainties. The algorithm finds all the ore
151 samples that are plotting inside the sample convex hull. The benefit of testing each potential
152 ore against the convex hull of the sample set, and not the other way around (Longman et al.
153 2018), which would amount to testing each sample against geographic groups of ores with
154 consistent Pb isotope compositions, is that the sample hull is robustly defined by high-
155 precision data. The downside of the convex hull approach is that some ore districts are over-
156 represented in the database with data variability at a given site being not specifically
157 considered. It is clear that the database contains an inordinate amount of Lavrion samples, yet
158 the hit maps are different for different samples (Gentelli et al. 2021, and this work). The effect
159 of unequal sample representativeness for densely populated mine fields could be adjusted by
160 normalizing the number of hits to sample density, but such a correction would make little
161 sense for isolated ores with a very small number of samples, such as mines in Iran and North
162 Africa. Rather, careful manual examination of local densities of individual hits will limit such
163 potential bias as has been shown by a previous application of the convex hull method to
164 multiple Iron Age *hacksilber* hoards (Gentelli et al. 2021) which showed no false-positive
165 identifications of bullion sources. Each Pb isotope datum extracted from a ca. 6700-entry
166 database on galena samples encompassing Europe, North Africa, and Western Asia is then
167 tested for inclusion in the convex hull. Data from major copper ore deposits, such as those
168 found in Cyprus and the Iberian Pyrite Belt, are unlikely to be significant Ag sources and

169 hence were left out from the search. **Figure 2** shows the position of the ores comprising the
170 database. An ore found to be included is considered a hit and therefore a potential Pb source,
171 whereas ores plotting outside the hull (considered a miss) can be safely excluded as potential
172 Pb sources. In order to minimize analytical errors and mass-dependent fractionation of Pb in
173 ores, we opted for using ^{206}Pb -standardized ratios, i.e., $^{204}\text{Pb}/^{206}\text{Pb}$, $^{207}\text{Pb}/^{206}\text{Pb}$, and
174 $^{208}\text{Pb}/^{206}\text{Pb}$. The hit densities are finally contoured on a geographic map shown in **Fig. 3** for
175 Greek silver coins, *alexanders*, and *sigloi*. **Figures 4 and 5** show the raw Pb isotopic
176 compositions of the hits identified by the convex hull approach on a grid of Pb model ages
177 and $^{238}\text{U}/^{204}\text{Pb}$ ($T_{\text{mod}}-\mu$) values in $^{207}\text{Pb}/^{204}\text{Pb}$ - $^{206}\text{Pb}/^{204}\text{Pb}$ space. A grid of Pb model ages and
178 $^{232}\text{Th}/^{238}\text{U}$ ($T_{\text{mod}}-\kappa$) values was not added to the $^{208}\text{Pb}/^{204}\text{Pb}$ - $^{206}\text{Pb}/^{204}\text{Pb}$ plot as this would
179 require adopting a single μ value for all samples which would be incorrect. A single grid
180 could instead have been drawn using the $T_{\text{mod}}-(\mu*\kappa)$ doublet, but this would be much less
181 informative.

4. Results and discussion

184 The coin Pb isotope data are listed in Table S1 (*Supplementary Information*). Figure 3 shows
185 the distribution of Pb ores consistent with the present results on coins, i.e., falling within the
186 convex hull of the data set, with histograms of model ages as insets.

187
188 First, cluster analysis was applied to the samples using techniques implemented by
189 commercial (Matlab) or public domain (R) packages (Albarède et al. 2021) (Fig. 1c). Each
190 coinage is satisfactorily accounted for by two clusters, which also stand out as separated
191 peaks in the histograms of model ages (Fig. 3, insets), though one of the clusters identified by
192 *sigloi* has only two elements, which is not enough for a convex hull to be defined in the 3D
193 space of Pb isotope compositions. The various Greek silver coins used for reference
194 emphasize the diversity of ore provenance but with a predominance from Lavrion. Some
195 districts, such as northwestern Sardinia, show more hits, which are consistent with evidence
196 of Sardinian silver sources identified in one Levant hoard of *hacksilber* (Eshel et al. 2019;
197 Gentili et al. 2021). Delile et al. (2019) suggested that Tunisian silver sources may have been
198 overlooked by ancient literature and explain the surprisingly fast revival of the Carthage
199 economy after the crushing defeat of the Second Punic War and the ensuing war penalties.
200 More isolated points, typically located in Gaul and Britain cannot be formally discounted, but
201 have not been proven so far to be significant silver producers. The Cévennes in southern

202 France (Munteanu et al. 2016; Ploquin et al. 2010), the British Pennines (Raistrick and
1 203 Jennings 1983), and Germany (Körlin 2006) also show evidence of ancient silver mining
2 204 activity, but no records exist to document that any of these regions produced significant
3 205 amounts of silver before Roman times. For both *sigloi* and *alexanders*, the hits are
4 206 concentrated around the Aegean and include Sifnos, Lavrion, Macedonia, and Thrace (red
5 207 fields in Fig. 3). For the 18 *sigloi*, Lavrion and Sifnos define a coherent hot spot. As expected,
6 208 Macedonia is also an important bullion source for *alexanders*. These results highlight the
7 209 major mining districts that made Athenian and Macedonian political and military successes
8 210 possible.
9 211

10 212 The Pangaeon area in Macedonia was already extensively mined when the Persians conquered
11 213 and controlled this area for a third of a century (512-479 BCE). Their one-time presence in
12 214 the west prompted large productions which would fade with the battle of Salamis and the
13 215 Persian retreat after the Second Invasion of Greece. Bresson (Bresson 2015; Bresson 2020)
14 216 estimates the yearly production of Lavrion, Thrace, and northern Greece to 1500 talents.
15 217 Callataÿ (2016) used die studies to raise the total amount of bullion to 10,000 talents (260
16 218 tons). How much silver extracted from other localities contributed indirectly, i.e., by trade or
17 219 military movements, is not clear. A likely scenario now emerges in which Persians, who
18 220 defeated the Lydians in 547 BCE and from then onwards were in contact with monetized
19 221 precious metals, took full advantage of the silver extraction and minting processes once they
20 222 became masters of the Pangaeon area. Following the retreat of the Persians from Europe after
21 223 the Second Invasion, the Achaemenid economy returned to the normal standard of the time in
22 224 Babylonia and other parts of the empire, which was to use silver for payment but largely in its
23 225 unminted form (Jursa 2010).
24 226

25 227 On the Indian side, Gandhara and Kamboja *shatamanas* (1827 hits) show an extreme scatter
26 228 in Pb isotopic compositions. Model ages fall into two groups (Fig. 6). One group with future
27 229 Pb model ages, which are mostly found in volcanic rocks, is missing from the record of East
28 230 Mediterranean ore deposits. The other group is characterized by positive Pb model ages (>100
29 231 Ma) but its large number of hits is clearly due to an extreme spread of the data in Pb isotope
30 232 space. From the British Isles to Spain, Greece, Turkey, and Iran, this group singles out no
31 233 specific province which could attest to a potential bullion provenance. The spread of the data,
32 234 and notably of model ages, in each group suggests the existence of multiple but modest
33 235 sources of Ag ores in the Middle East.
34
35
36
37
38
39
40
41
42
43
44
45
46
47
48
49
50
51
52
53
54
55
56
57
58
59
60
61
62
63
64
65

1
2 237 The outcome of the present work is twofold: the data on Persian *sigloi* show the prevalence of
3
4 238 metal components with the strong Pb isotopic signature of Laurion (Figure 4), while
5 239 *alexanders* further show additional Thraco-Macedonian, Thasos, Cycladic, and other
6
7 240 unknown sources (Figure 5). The possibility of sources in Tunisia remains enigmatic but may
8
9 241 also reflect some overlap with sources in Chalkidiki. The difference between *sigloi* and
10
11 242 *alexanders* suggest that *sigloi* were struck from local Ionian sources. The present isotopic data
12
13 243 complement the trace element data of Olivier et al. (2017) on *alexanders*. The comparison of
14
15 244 *alexander* Au/Ag and Pb/Ag data with those of archaic Greek coinage (Davis et al. 2020)
16 245 (Fig. 7) shows that *alexanders* are consistent with a mixture of gold-rich Thraco-Macedonian
17
18 246 and gold-depleted, lead-rich Attic sources. Given that in most cases Greek silver coins
19
20 247 retained a tight Pb isotope source signature, any mixing must have happened at a late stage.
21
22 248 Whether mixing should be assigned to bullion melting at the time of tribute collection, as
23
24 249 reported by Herodotus, or to reprocessing of the Persian treasury by Macedonians for minting
25
26 250 is still open to question. There is no necessity for Greek bullion to have journeyed directly
27
28 251 from Greece to Persia as formal tribute; intermediaries of all sorts over arbitrary time intervals
29
30 252 could have achieved the same result. Trade, war indemnities, and deposits in temples such as
31
32 253 Delphi or Ephesus efficiently redistributed silver all around the eastern Mediterranean. In this
33
34 254 respect, the case of Egypt, which according to Herodotus (III.91) had to pay its tribute partly
35
36 255 in silver (700 talents), while no silver mine is known in this area, is illuminating. Even if
37
38 256 Egypt, a country which benefitted from strong exports based on barley and wheat, could not
39
40 257 fully meet the Persian demand in silver, it is probable that at least part of the tribute must have
41
42 258 been paid in metal, both minted and unminted.

43
44 260 Although some west-east circulation of Greek and *sigloi* silver coins in the Achaemenid
45
46 261 empire is attested to in particular by the hoards of Kabul (Schlumberger 1953), Babylon
47
48 262 (Reade 1986), and Malayer, next to Ecbatana (Kraay and Moorey 1968), hoarding of Persian
49
50 263 *sigloi* in Persepolis and other major urban centers at the heart of the empire was uncommon
51
52 264 and an essentially ‘silverized’ but coin-less character of the Persian economy is usually
53
54 265 favored (Jursa 2010; Meadows 2005) with possible exceptions during the reign of Artaxerxes
55
56 266 III (Alram 2012). Additionally, Indian bent silver bars differ markedly in Pb isotopic
57
58 267 composition from the *sigloi* and the *alexanders*. Again, this is no surprise since neither
59
60 268 literary sources nor monetary circulation attested to by deposits indicate any flow of silver
61
62 269 from the far east to the center of the empire. As explained below, it should be noted that no
63
64
65

270 records exist for Achaemenid-era silver mines in either modern Iran, Afghanistan, Pakistan,
271 Turkmenistan, or India, or, if such records did exist, they have been lost. Although silver
272 extraction from Pb ores is mentioned for the Sassanid Period (224 AD-670 AD; Ghorbani
273 2013), the comparative chemistry of Parthian and Sassanid coinage is elusive about Persian
274 sources (Sodaei et al. 2013). In modern Iran, silver is mostly mentioned in connection with
275 gold and lead deposits (Ghorbani 2013), rarely in the form of silver ore. Porphyry copper
276 deposits are abundant in Iran (Zürcher et al. 2019), but because molten Ag is sparingly
277 soluble in Cu with which it forms a eutectic at 28.1 wt.% Cu (Subramanian and Perepezko
278 1993), the costly extraction of minor silver from copper ores simply may not have been
279 profitable. The US Geological Survey reports on Afghanistan ore deposits but does not flag
280 any significant silver-rich ores (Peters et al. 2011). The geologically old and otherwise
281 basaltic India is an unlikely source of silver and lead, but the recent discovery of the major
282 Huoshaoyun Zn-Pb deposit in the Karakorum Range (Li et al. 2019) suggests that sources of
283 silver and lead, now exhausted and unrecorded in the extant literature, may have existed to
284 support the manufacturing of early Indian coinage. Significant Asian sources of silver
285 contributing to the Achaemenid treasure therefore remain highly speculative.

286
287 Most silver used to strike both the silver *alexanders* and the Persian *sigloi* presumably came
288 from peri-Aegean metal sources. It is therefore appealing to consider that the Persian mix
289 reflects the tributes exacted from the Greeks or, indirectly, from other satrapies which traded
290 with the Greeks. Nevertheless, the Persian mix is occasionally found in hoards of *hacksilber*
291 buried in the Early Iron Age (11th-10th centuries BCE) in modern Israel (Eshel et al. 2019;
292 Gentelli et al. 2021). In addition, pollution of Alpine glaciers by Pb and Sb during the Iron
293 Age, both strong markers of silver metallurgy, is barely measurable compared to values
294 during the Roman era (Preunkert et al. 2019), which reflects that silver mining prior to the
295 Persian expansion of the 6th century BCE may have been insignificant. What is currently
296 defined as the Persian mix could also be a long-lived eastern Mediterranean mix dominated
297 by circum-Aegean sources, where most silver had already been melted again and again all the
298 way back to the Bronze Age.

299
300 We finally briefly speculate on why Persian kings hoarded bullion to an extent never seen at
301 any other time in antiquity. Unproductive bullion accumulation was certainly a common habit
302 of many societies, but the massive melting and underground storage of silver described by
303 Herodotus reached an unparalleled practice which deserves scrutiny. Beyond the Persian

304 treasuries, it is difficult to estimate the volume of silver used for transactions within the
1 305 Achaemenid empire, but it should not be minimized and transactions could have been taking
2 306 place as early as the 6th century BCE (Jursa 2011; Pirngruber 2017). As attested to by the
3 307 presence of chopped Greek coins in the Babylonian Rassam hoard from the end of the 4th
4 308 century BCE (Reade 1986), silver coinage clearly was not the prevalent form of currency in
5 309 the central part of the empire (Alram 2012; Le Rider 2001). The silver shekel, next to barley
6 310 and other in-kind commodities, nevertheless certainly was present both physically and as a
7 311 unit of account (Jursa 2011; Powell 1996; van der Spek et al. 2018). The noticeable price
8 312 deflation observed in Babylonia during the 5th and 4th centuries BCE was assigned to
9 313 intensified captation of silver through taxes (Stolper 1985), but demography and improvement
10 314 of cash-crop agriculture may also have been important alternative factors (Monerie 2013).
11 315 Using concepts from modern mainstream economics, which were almost certainly not part of
12 316 the Persian culture, massive hoarding resulted in a much longer bullion residence time in
13 317 royal treasuries and was effective at slowing down large-scale bullion circulation. The
14 318 clamping down on silver supply, in both its minted and unminted forms, combined with the
15 319 massive silver tributes imposed on subjugated societies, which were otherwise allowed to
16 320 keep their political system, drained regional silver resources on a massive scale into the royal
17 321 treasury. If tribute was an efficient way of drawing off silver accumulated by potential
18 322 adversaries such as Egypt and Ionian Greece, long-distance trade was the long arm of this
19 323 scheme, certainly cheaper and less risky than launching distant military campaigns.
20 324 Considering that the much-coveted Greek hoplites were usually paid in silver and gold coins,
21 325 a major side effect of this policy must have been that it helped render the recruiting of large
22 326 mercenary forces a royal privilege (Bresson 2020), thereby reducing the threats, both
23 327 domestic and abroad, to the throne. But eventually, the systematic storage of very large
24 328 amounts of silver in the royal vaults, whether intentional or not, contributed to the collapse of
25 329 the Persian empire and ushered in its replacement by the Hellenistic kingdoms of Antigonid
26 330 Macedonia and Ptolemaic Egypt, and by the Seleucid empire in the East.
27 331

51 332 **5. Conclusions**

52 333 The Achaemenids' ruling of old Persia achieved the largest accumulation of precious metals
53 334 reported in ancient history, equivalent to about 5,000 metric tons of silver. While research has
54 335 shown how Alexander the Great and his successors processed these gigantic quantities by
55 336 striking coins, the origins of the silver have so far remained largely unknown. Lead isotope
56 337 abundances determined in this work on both Persian and Alexander silver coinages trace the
57
58
59
60
61
62
63
64
65

338 bullion sources to the southern Aegean, Macedonia, and Thrace, while lead from pseudo-
339 coinage from early Indian kingdoms is markedly different from the rest, hence excluding
340 India as a source. Fully understanding how and when such huge amounts of Aegean silver
341 were extracted and eventually arrived in the Persian treasuries is emerging as a new challenge
342 for future studies.

344 **Acknowledgments**

345 This work is a contribution of Advanced Grant 741454-SILVER-ERC-2016-ADG ‘Silver
346 Isotopes and the Rise of Money’ awarded to FA by the European Research Council (ERC).
347 We thank Marine Pinto, Chloé Malod-Dognin, and Liesel Gentelli for help with analytical
348 work and coin data compilation, and Katrin Westner, Tzilla Eshel, and Yigal Erel for useful
349 discussions. Two anonymous reviewers are gratefully acknowledged for their constructive
350 comments and Editor Yannis Bassiakos for his efficient handling of our submission.

352 **Author statements**

- 353 • The authors have no competing conflicts of interest to disclose.
- 354 • Data sharing plan: The data in Table S1 (*Supplementary Information*) will be made
355 fully available upon acceptance of the manuscript.

357 **Author contributions**

358 JBT and FA designed the research and wrote the paper with input from FdC; FA selected the
359 coins for purchase; JBT produced the Pb isotope data with assistance from technical staff; PT
360 ensured instruments were working.

362 **References**

- 363 Albarède F., Blichert-Toft J., de Callataÿ F., Davis G., Debernardi P., Gentelli L., Gitler H.,
364 Kemmers F., Klein S., Malod-Dognin C. (2021) From commodity to money: The rise of
365 silver coinage around the Ancient Mediterranean (sixth–first centuries bce).
366 *Archaeometry* 63(1):142-155
- 367 Albarede F., Desaulty A.M., Blichert-Toft J. (2012) A geological perspective on the use of Pb
368 isotopes in Archaeometry. *Archaeometry* 54(5):853-867
- 369 Albarede F., Juteau M. (1984) Unscrambling the lead model ages. *Geochim Cosmochim Acta*
370 48(1):207-212
- 371 Alram M. (1993) Dareikos und Siglos: Ein neuer Schatzfund achaimenidischer Sigloi aus
372 Kleinasien. *Res Orientales* 5:23-53
- 373 Alram M. (2012) The coinage of the Persian Empire. In: Metcalf W.E. (ed) *The Oxford*
374 *Handbook of Greek and Roman Coinage*, vol. Oxford University Press, Oxford, pp 61-87

- 375 Armayor O.K. (1978) Herodotus' Catalogues of the Persian Empire in the light of the
1 376 monuments and the greek literary tradition. *Transactions of the American Philological*
2 377 *Association* (1974-) 108:1-9
- 3 378 Blichert-Toft J., Delile H., Lee C.T., Stos-Gale Z., Billström K., Andersen T., Hannu H.,
4 379 Albarède F. (2016) Large-scale tectonic cycles in Europe revealed by distinct Pb isotope
5 380 provinces. *Geochemistry, Geophysics, Geosystems* 17(10):3854-3864
- 7 381 Bresson A. (2015) *The making of the ancient Greek economy: Institutions, markets, and*
8 382 *growth in the city-states*. Princeton University Press,
- 9 383 Bresson A. (2020) Silverization, prices, and tribute in the Achaemenid empire. In: Tuplin
10 384 C.J., Ma J. (eds) *Aršāma and his World The Bodleian Letters in Context Vol III*, vol.
12 385 Oxford Univ. Press, Oxford, pp 209-248
- 13 386 Callatay F.d. (1989) Les trésors achéménides et les monnayages d'Alexandre: espèces
14 387 immobilisées et espèces circulantes? *Revue des études anciennes* 91(1):259-274
- 15 388 Callatay F.d. (1993) Le monde grec hellénistique. In: Callatay F.d., Depeyrot G., Villaronga
16 389 L. (eds) *L'argent monnayé d'Alexandre le Grand à Auguste* Brussels, vol. Cercle d'études
18 390 numismatiques, Bruxelles, pp 13-46
- 19 391 Callatay F.d. (2016) Putting Southern Aegean coinages in perspective. In: Kerstin
20 392 Höghammar Symposium, vol., Uppsala
- 22 393 Davis G., Gore D.B., Sheedy K.A., Albarède F. (2020) Separating silver sources of Archaic
23 394 Athenian coinage by comprehensive compositional analyses. *Journal of Archaeological*
24 395 *Science* 114:105068
- 25 396 Delile H., Mazzini I., Blichert-Toft J., Goiran J.-P., Arnaud-Godet F., Salomon F., Albarède
26 397 F. (2014) Geochemical investigation of a sediment core from the Trajan basin at Portus,
28 398 the harbor of ancient Rome. *Quaternary Science Reviews* 87:34-45
- 29 399 Delile H., Pleuger E., Blichert-Toft J., Goiran J.-P., Fagel N., Gadhoun A., Abichou A.,
30 400 Jerbania I.B., Fentress E., Wilson A.I. (2019) Economic resilience of Carthage during the
31 401 Punic Wars: Insights from sediments of the Medjerda delta around Utica (Tunisia).
32 402 *Proceedings of the National Academy of Sciences* 116(20):9764-9769
- 34 403 Eckrich C.A., Albeke S.E., Flaherty E.A., Bowyer R.T., Ben-David M. (2020) rKIN: Kernel-
35 404 based method for estimating isotopic niche size and overlap. *Journal of Animal Ecology*
36 405 89(3):757-771
- 37 406 Eshel T., Erel Y., Yahalom-Mack N., Tirosh O., Gilboa A. (2019) Lead isotopes in silver
38 407 reveal earliest Phoenician quest for metals in the west Mediterranean. *Proceedings of the*
40 408 *National Academy of Sciences* 116(13):6007-6012
- 41 409 Gentelli L., Blichert-Toft J., Davis G., Gitler G., Gitler H., Albarede F. (2021) Metal
42 410 provenance of Late Bronze to Iron Age Hacksilber hoards in the southern Levant. *Journal*
43 411 *of Archaeological Sciences* 134:105472 doi:<https://doi.org/10.1016/j.jas.2021.105472>
- 45 412 Ghorbani M. (2013) *Economic geology of Iran*. Springer,
- 46 413 Holt F.L. (2016) *The treasures of Alexander the Great: how one man's wealth shaped the*
47 414 *world*. Oxford University Press,
- 48 415 Jursa M. (2010) Aspects of the economic history of Babylonia in the first millennium BC.
49 416 *Economic geography, economic mentalities, agriculture, the use of money and the*
51 417 *problem of economic growth*:119
- 52 418 Jursa M. (2011) Taxation and Service Obligations in Babylonia from Nebuchadnezzar to
53 419 Darius and the Evidence for Darius' Tax Reform. In: Rollinger R., Truschnegg B.,
54 420 Bichler R. (eds) *Taxation and service obligations in Babylonia from Nebuchadnezzar to*
55 421 *Darius and the evidence for Darius' tax reform*, vol. Wiesbaden, Harrassowitz Verlag, pp
56 422 431-448
- 58 423 Körlin G. (2006) Römischer Bergbau auf dem Lüderich bei Rösrath, Rheinisch-Bergischer
59 424 Kreis. Köhne R, Reininghaus W, Stöllner Th (eds) *Bergbau im Sauerland Westfälischer*

- 425 *Bergbau in der Römerzeit und im frühen Mittelalter Schriften der Historischen*
1 426 *Kommission für Westfalen* 20:21-31
- 2 427 Kraay C.M., Emeleus V.M. (1962) The Composition of Greek Silver Coins: analysis by
3 428 neutron activation.
- 4 429 Kraay C.M., Moorey P.R.S. (1968) Two fifth century hoards from the Near East. *Revue*
5 430 *numismatique* 6(10):181-235
- 6 431 Le Rider G. (2001) *La naissance de la monnaie: pratiques monétaires de l'Orient ancien.*
7 432 Presses Universitaires de France-PUF,
- 8 433 Li H., Xu X.-W., Borg G., Gilg H.A., Dong L.-H., Fan T.-B., Zhou G., Liu R.-L., Hong T.,
9 434 Ke Q. (2019) Geology and Geochemistry of the giant Huoshaoyun zinc-lead deposit,
10 435 Karakorum Range, northwestern Tibet. *Ore Geology Reviews* 106:251-272
- 11 436 Longman J., Veres D., Ersek V., Phillips D.L., Chauvel C., Tamas C.G. (2018) Quantitative
12 437 assessment of Pb sources in isotopic mixtures using a Bayesian mixing model. *Scientific*
13 438 *Reports* 8(1):6154 doi:10.1038/s41598-018-24474-0
- 14 439 Meadows A. (2014) The spread of coins in the Hellenistic world. In: *Explaining Monetary*
15 440 *and Financial Innovation*, vol. Springer, pp 169-195
- 16 441 Meadows A.R. (2005) The administration of the Achaemenid Empire. *Forgotten Empire: The*
17 442 *world of ancient Persia*:181-209
- 18 443 Milot J., Malod-Dognin C., Blichert-Toft J., Télouk P., Albarède F. (2021) Sampling and
19 444 combined Pb and Ag isotopic analysis of ancient silver coins and ores. *Chemical Geology*
20 445 564:120028
- 21 446 Monerie J. (2013) Aspects de l'économie de la Babylonie aux époques hellénistique et parthe
22 447 (IVe S. av J.-C.-IerS. av J.-C.). *Unpublished PhD thesis, Université Paris I–Panthéon-*
23 448 *Sorbonne Paris*
- 24 449 Munteanu G., Kammenthaler E., Maintenant J., Rico C., Fabre J.-M., Beyrie A. (2016) Le
25 450 complexe minier gaulois des Barrenes (Aude, France) dans son contexte géologique et
26 451 minéralogique. *ArcheoSciences Revue d'archéométrie* (40):163-180
- 27 452 Nicolet C. (1984) Pline, Paul et la théorie de la monnaie. *Athenaeum* 62:105
- 28 453 Olivier J., Duyrat F., Carrier C., Blet-Lemarquand M. (2017) Minted Silver in the Empire of
29 454 Alexander. In: *Alexander the Great, a Linked Open World*, vol 116. Ausonius Éditions,
30 455 pp 127–146
- 31 456 Peters S.G., King T.V., Mack T.J., Chornack M.P. (2011) *Summaries of Important Areas of*
32 457 *Mineral Investment and Production Opportunities of Nonfuel Minerals in Afghanistan.*
33 458 US Department of the Interior, US Geological Survey,
- 34 459 Pirngruber R. (2017) *The economy of late Achaemenid and Seleucid Babylonia.* Cambridge
35 460 University Press,
- 36 461 Ploquin A., Allée P., Bailly-Maître M.-C., Baron S., De Beaulieu J.-L., Carignan J., Laurent
37 462 S., Lavoie M., Le Carlier C.M., Paradis S. (2010) PCR–Le plomb argentifère ancien du
38 463 Mont Lozère (Lozère). A la recherche des mines, des minerais et des ateliers, des
39 464 paysages et des hommes. *ArcheoSciences Revue d'archéométrie* (34):99-114
- 40 465 Powell M. (1996) Money in Mesopotamia. *Journal of the Economic and Social History of the*
41 466 *Orient* 39(3):224-242
- 42 467 Preunkert S., McConnell J.R., Hoffmann H., Legrand M., Wilson A.I., Eckhardt S., Stohl A.,
43 468 Chellman N.J., Arienzo M.M., Friedrich R. (2019) Lead and antimony in basal ice from
44 469 Col du Dome (French Alps) dated with radiocarbon: A record of pollution during
45 470 antiquity. *Geophysical Research Letters* 46(9):4953-4961
- 46 471 Raistrick A., Jennings B. (1983) *A history of lead mining in the Pennines.* George Kelsall,
47 472 Littleborough
- 48 473 Reade J. (1986) A hoard of silver currency from Achaemenid Babylon. *Iran* 24(1):79-87
- 49
50
51
52
53
54
55
56
57
58
59
60
61
62
63
64
65

- 474 Reddy D.R. (2014) The Emergence and Spread of Coins in Ancient India. In: *Explaining*
 1 475 *Monetary and Financial Innovation*, vol. Springer, pp 53-77
- 2 476 Robinson J.R. (2021) Investigating isotopic niche space: using rkin for stable isotope studies
 3 477 in Archaeology. *Journal of Archaeological Method and Theory* doi:10.1007/s10816-
 4 478 021-09541-7
- 5 479 Schlumberger D. (1953) L'argent grec dans l'Empire achéménide. In: Curiel R., Schlumberger
 6 480 D. (eds) *Trésors monétaires d'Afghanistan*, vol. Klincksieck, Paris, pp 199-222
- 7 481 Sodaei B., Hajivaliei M., Nadooshan F.K. (2013) Possible sources for extraction of silver by
 8 482 comparison of Parthian and Sasanian coins in Mede satraps. *Mediterranean Archaeology*
 9 483 *& Archaeometry* 13(1)
- 10 484 Stolper M.W. (1985) *Entrepreneurs and Empire: The Murašû Archive, the Murašû Firm, and*
 11 485 *Persian Rule in Babylonia*. Nederlands historisch-archaeologisch instituut,
- 12 486 Stos-Gale Z.A., Gale N.H. (2009) Metal provenancing using isotopes and the Oxford
 13 487 archaeological lead isotope database (OXALID). *Archaeological and Anthropological*
 14 488 *Sciences* 1(3):195-213
- 15 489 Subramanian P., Perepezko J. (1993) The Ag-Cu (silver-copper) system. *Journal of Phase*
 16 490 *Equilibria* 14(1):62-75
- 17 491 Tuplin C. (2014) The Changing Pattern of Achaemenid Persian Royal Coinage. In:
 18 492 *Explaining Monetary and Financial Innovation*, vol. Springer, pp 127-168
- 19 493 van der Spek R., Dercksen J., Kleber K., Jursa M. (2018) Money, silver and trust in
 20 494 Mesopotamia. In: van der Spek R., van Leeuwen B. (eds) *Money, Currency and Crisis:*
 21 495 *In Search of Trust, 2000 BC to AD 2000*, vol. Routledge, London, pp 102-131
- 22 496 Van der Spek R., van Leeuwen B. (2014) Quantifying the Integration of the Babylonian
 23 497 Economy in the Mediterranean World Using a New Corpus of Price Data, 400-50 BC.
 24 498 *Long-term quantification in ancient history*:79-102
- 25 499 Westner K.J., Birch T., Kemmers F., Klein S., Höfer H.E., Seitz H.-M. (2020) Rome's rise to
 26 500 power. Geochemical analysis of silver coinage from the Western Mediterranean (4th to
 27 501 2nd centuries BCE). *Archaeometry* 62(3):577-592 doi:10.1111/arc.12547
- 28 502 Zürcher L., Bookstrom A.A., Hammarstrom J.M., Mars J.C., Ludington S., Zientek M.L.,
 29 503 Dunlap P., Wallis J. (2019) Tectono-magmatic evolution of porphyry belts in the central
 30 504 Tethys region of Turkey, the Caucasus, Iran, western Pakistan, and southern Afghanistan.
 31 505 *Ore Geology Reviews* 111:102849
- 32 506

40 507 **Figure captions**

41 508 **Figure 1.** (a) Source identification with Pb isotopes in 2- and 3-dimensional plots may
 42 509 provide different outcomes. The symbol P represents a single data point in 3D Pb isotope
 43 510 space and P_{xy} , P_{xz} , and P_{yz} its three 2D projections onto the three xy, xz, and yz faces
 44 511 (conventional isotope diagrams). The lavender 3D field f represents a single mining district
 45 512 and the light-grey fields f_{xy} , f_{xz} , and f_{yz} its three 2D projections. Clearly, inclusion of a point in
 46 513 one and even two of these 2D fields is not sufficient to establish that P is part of the 3D f
 47 514 field. It should therefore not be concluded that the inclusion of a data point in a common field
 48 515 in 2D representation demonstrates that it belongs to the same field in 3D. (b) The convex hull
 49 516 technique for calculating the closest convex circumscribing volume to a set of points in a 3-
 50 517 dimensional space. This volume, here in yellow for an arbitrary set of data, is defined by all

518 the x, y, z triplets of Pb isotope ratios of the sample (e.g., alexanders or sigloi). ‘Hits’ are the
1 519 localities of the samples extracted from a ca. 6700-entry database on galenas which plot
2 520 within the convex hull. (c) The four steps used in this work to identify the ore deposits which
3 521 are ‘hits’ in the convex hulls defined by the samples. For purpose of illustration and
4 522 readability, this sketch of the different steps was drawn as a 2-dimensional representation
5 523 though all steps were carried out in three dimensions in the present work. The variables x and
6 524 y stand for any arbitrary Pb isotope ratios. Step 1: samples (yellow circles, e.g., sigloi) are
7 525 plotted in an x-y representation; step 2: standard cluster analysis is carried out and, in this
8 526 case, identifies two groups shown within dotted contours; step 3: convex hulls are calculated
9 527 for each group with a small allowance (in grey) added for the fringe of each hull to take
10 528 analytical uncertainties into account; step 4: the position of each ore sample inside (hits
11 529 shown with green crosses) or outside (misses shown with red crosses) the convex hull is
12 530 determined numerically (fringe not shown). In the present study, the number of groups vary
13 531 between 1 and 2.

532

27 533 **Figure 2.** Map showing the localities of the ores listed in the ca. 6700-entry Pb isotope
28 534 database on galena samples used with the convex hull algorithm of this study. The database is
29 535 an extension of that published by Blichert-Toft et al. (2016) with copper and zinc ore and
30 536 artefact data removed. Sample locations have been randomly jittered in a circle of
31 537 0-0.2 degree (0-22 km) radius around the true coordinates to increase their apparent spread
32 538 and provide a better vision of sample distribution.

539

40 540 **Figure 3.** Maps of the Pb isotope ‘hits’ observed for sigloi (bottom panel), alexanders (middle
41 541 panel), and Greek silver coins (top panel) using the convex hull algorithm. The histograms of
42 542 model ages (insets) show how well grouped the results are. The total number of hits is the
43 543 number of matches between coin and ore Pb isotopic compositions. The Pb ore database
44 544 consists of about 6700 European, North African, and Middle Eastern ores significantly
45 545 expanded and updated from a smaller core of data on Pb ores initially compiled in the
46 546 OXALID database (Stos-Gale and Gale 2009) after careful removal of artefacts, slags, and Cu
47 547 ores. Isolated hits (cyan-colored symbols) may reflect minor production sites, but may also
48 548 reflect analytical issues and local geological intricacies; they are not localities where
49 549 substantial silver production has ever been documented and hence are considered as
50 550 fortuitous. Red-shaded fields represent areas with a hit density >10% per degree-squared
51 551 normalized to the entire population of hits, which attest to the most frequent provenances.

61
62
63
64
65

552 *Sigloi* are therefore dominated by Attic and peri-Attic silver (Siphnos, Milos), with
553 *alexanders* including additional Thracο-Macedonian sources.

554

555 **Figure 4.** Plot of the hits obtained for *sigloi*. In the 3-dimensional space of Pb isotopic ratios,
556 two clusters are first identified by cluster analysis. One of them comprises only two points
557 and hence no convex hull can be calculated. The convex hull of the second cluster shows hits
558 largely dominated by Laurion lead. Convex hulls are expanded by 5% to take analytical
559 uncertainties into account. The samples labelled ‘Tunisia’ may indicate that silver from the
560 Carthage hinterland has been neglected by ancient literature (Delile et al. 2019) or that other
561 fields, such as Chalkidiki, were poorly sampled for Pb isotopic analysis. The ‘other’ group
562 represents isolated Pb mines insufficiently documented by Pb isotope analysis. The model age
563 isochrons and the growth curves for different μ values calculated with Albarède and Juteau’s
564 (1984) parameters are shown for reference in the bottom panel.

565

566 **Figure 5.** Plot of the hits obtained for the analyzed *alexanders*. As in Figure 4, two clusters
567 are identified. The convex hull of the cluster with Pb older model ages represent poorly
568 documented mines from unexpected localities in Gaul, Britain, and Asia Minor. The cluster
569 with younger model ages point to the Cyclades, Thasos, Chalkidiki, and Rhodope. As in Fig.
570 4, the model age isochrons and the growth curves for different μ values calculated with
571 Albarède and Juteau’s (1984) parameters are shown for reference in the bottom panel.

572

573 **Figure 6.** Comparison of the Pb model ages (in million years, Ma) of the four data sets
574 analyzed in this work. Model ages represent the apparent tectonic age of the Pb ores used for
575 silver cupellation (Albarede et al. 2012). Negative model ages are found only in mantle-
576 derived volcanics. With a few exceptions, silver from Indian Gandhara and Kamboja
577 *shatamanas* does not seem to have been a significant component of the ‘Persian mix’ used by
578 Alexander and his successors to mint their coinage.

579

580 **Figure 7.** Triangular plot of Cu-Au-Pb concentrations in pre- (Philip II, in blue) and post-330
581 BCE (Alexander and Philip III, in red) Macedonian coinage (Olivier et al. 2017). The
582 background contours represent concentration frequencies in ca. 1200 archaic Greek coins and
583 delimit the Au-rich Thracο-Macedonian field and the Pb-rich Attica field (Davis et al. 2020).
584 Note the low Cu contents of Macedonian coinage. Macedonian silver coinage is a mixture of
585 Au-rich Thracο-Macedonian and Pb-rich Attic sources.

61
62
63
64
65

586

1
2 587 **Table captions**

3 588 **Table S1.** (Supplementary Information). Pb isotopic ratios and model parameters.
4
5
6
7
8
9
10
11
12
13
14
15
16
17
18
19
20
21
22
23
24
25
26
27
28
29
30
31
32
33
34
35
36
37
38
39
40
41
42
43
44
45
46
47
48
49
50
51
52
53
54
55
56
57
58
59
60
61
62
63
64
65

Figure 1

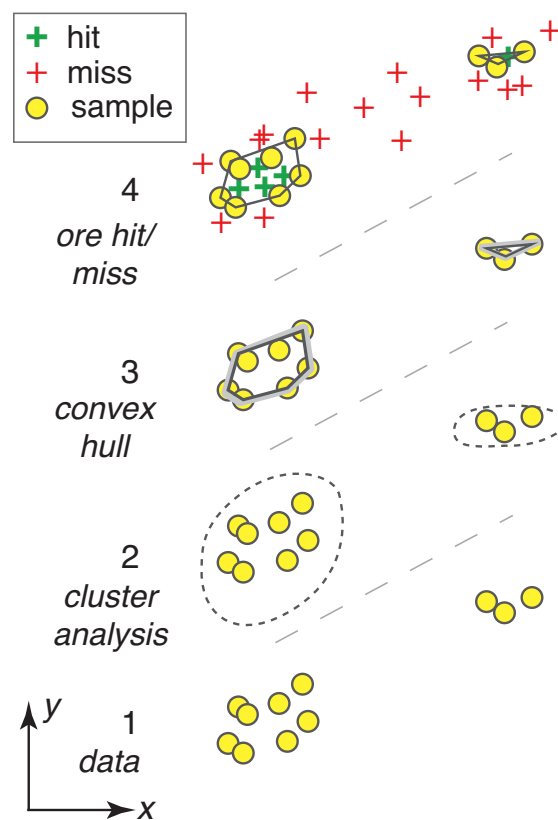
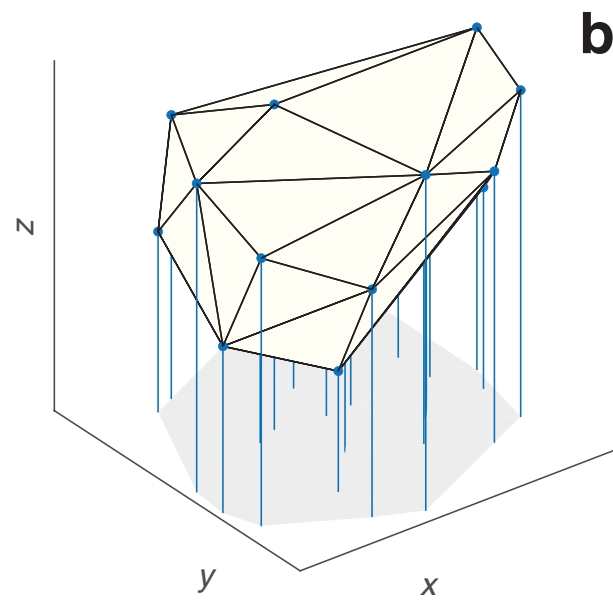
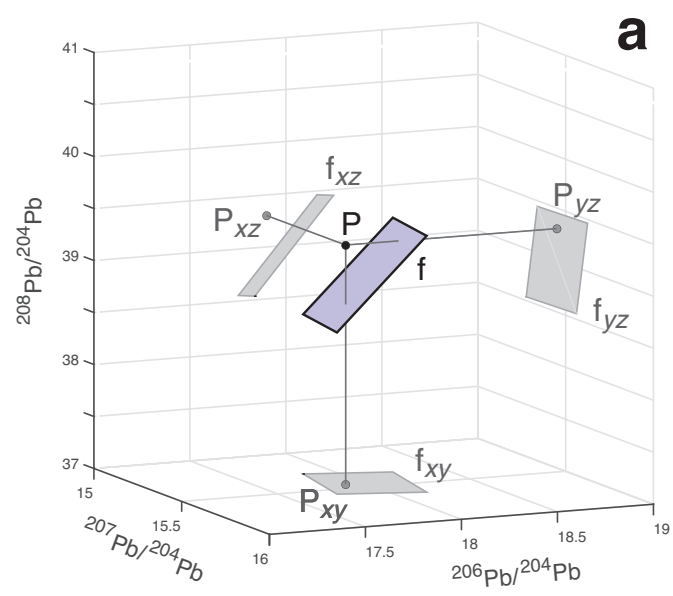


Figure 2

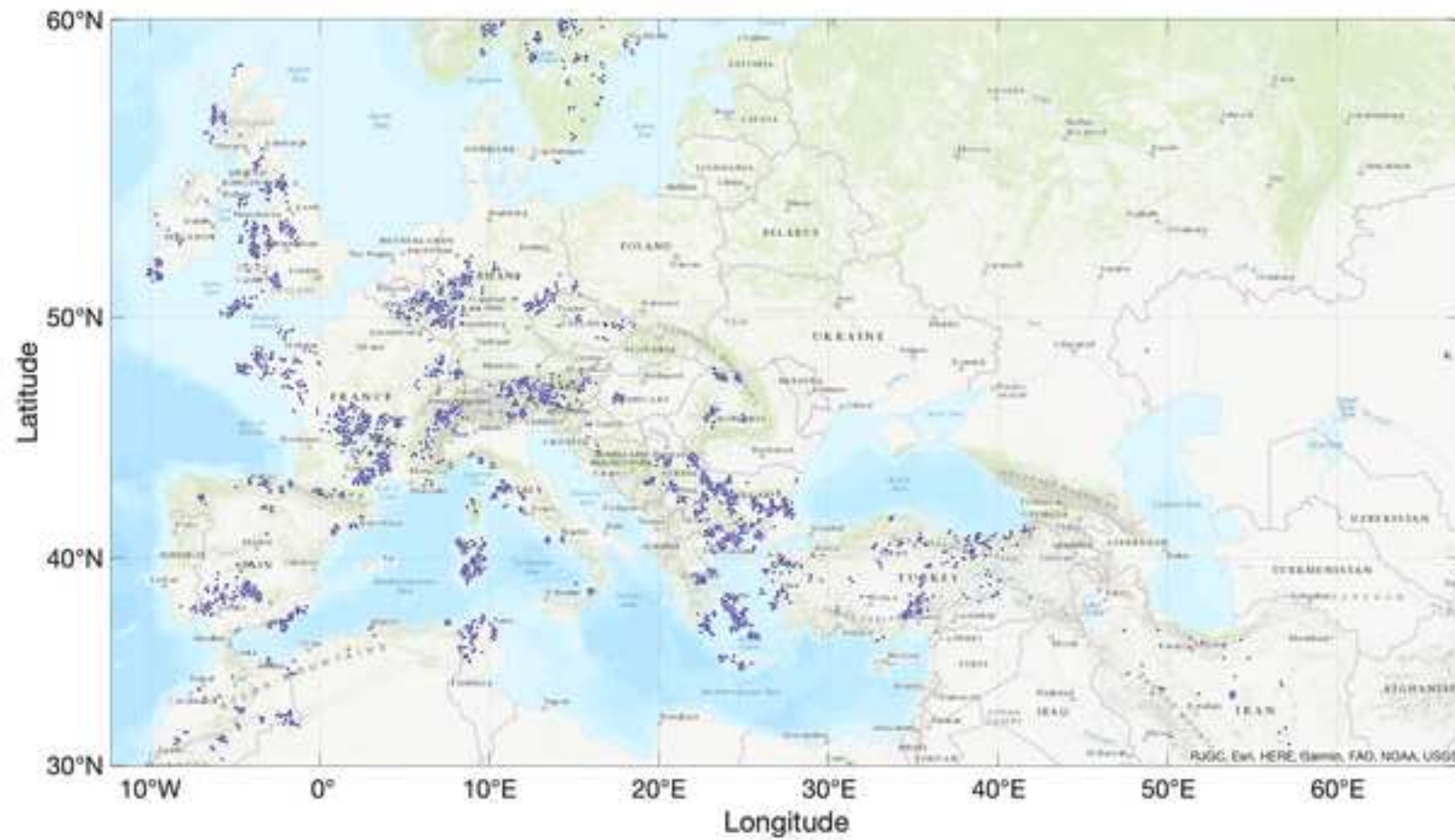
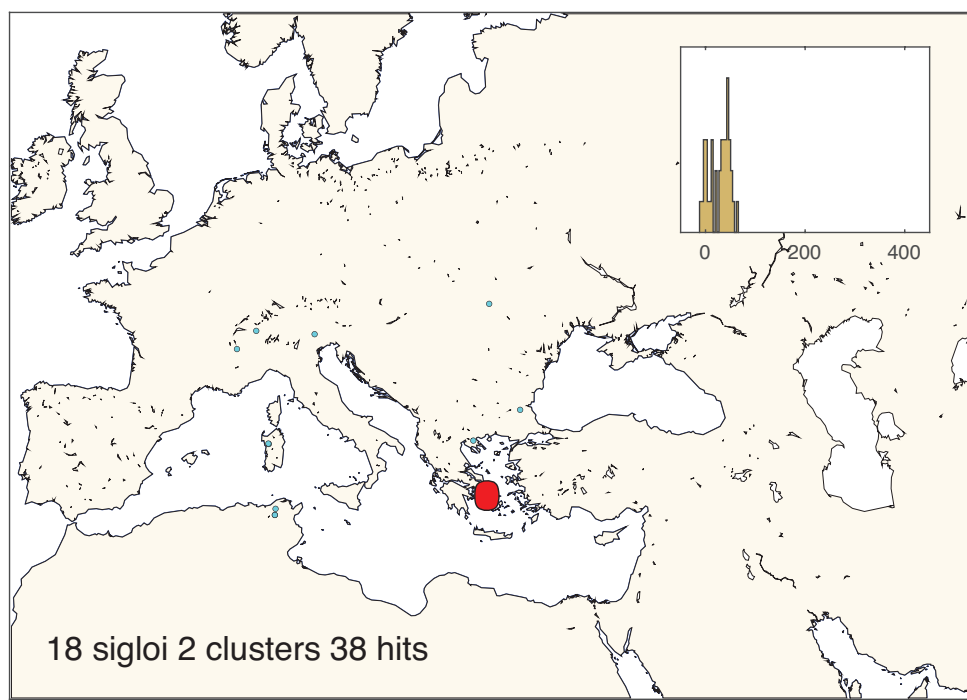
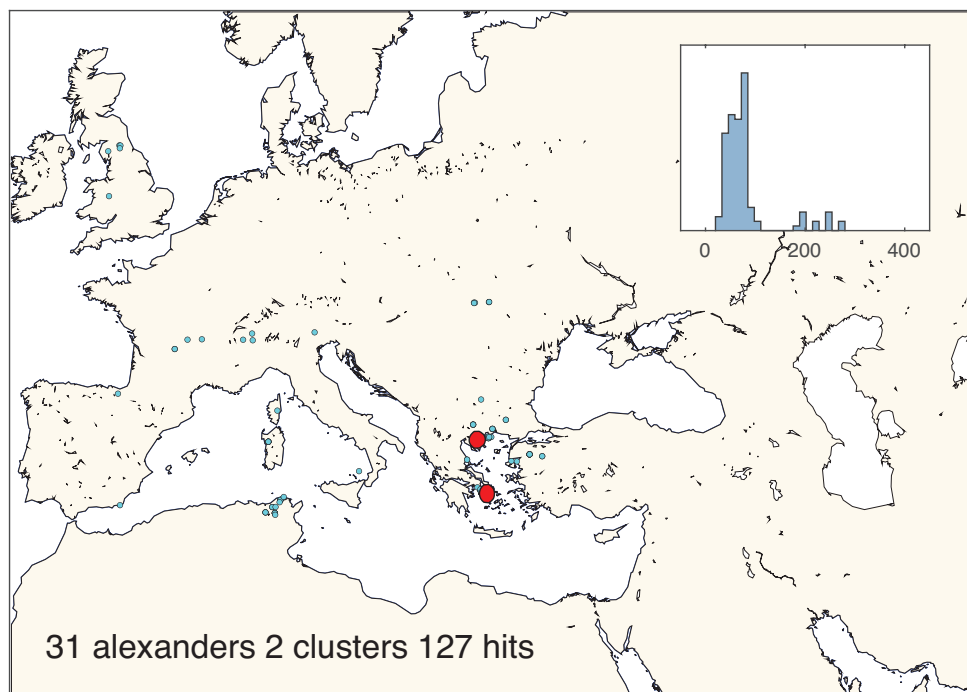
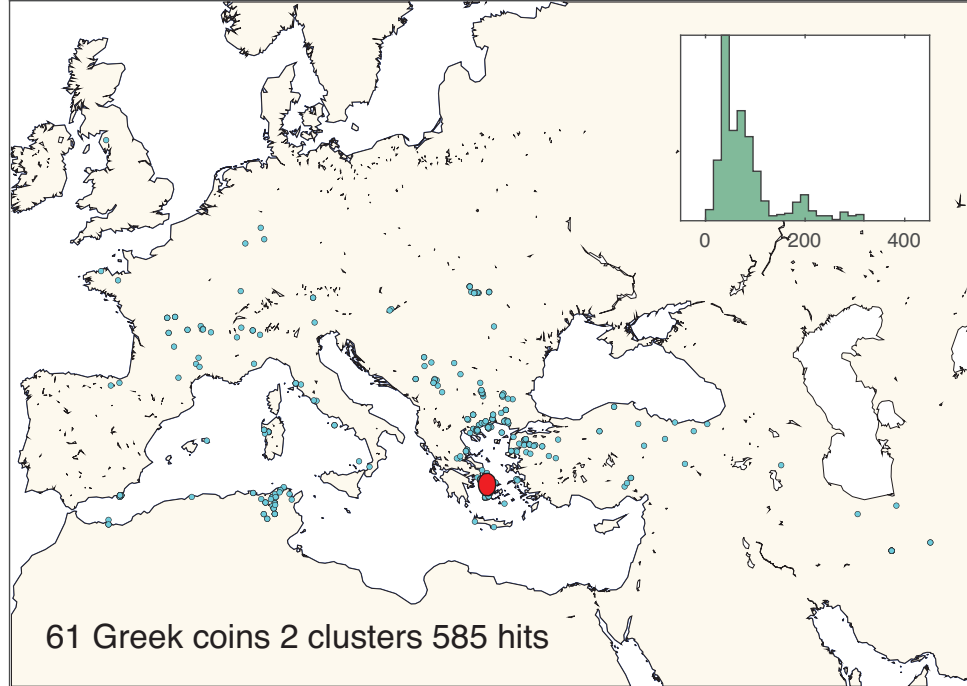
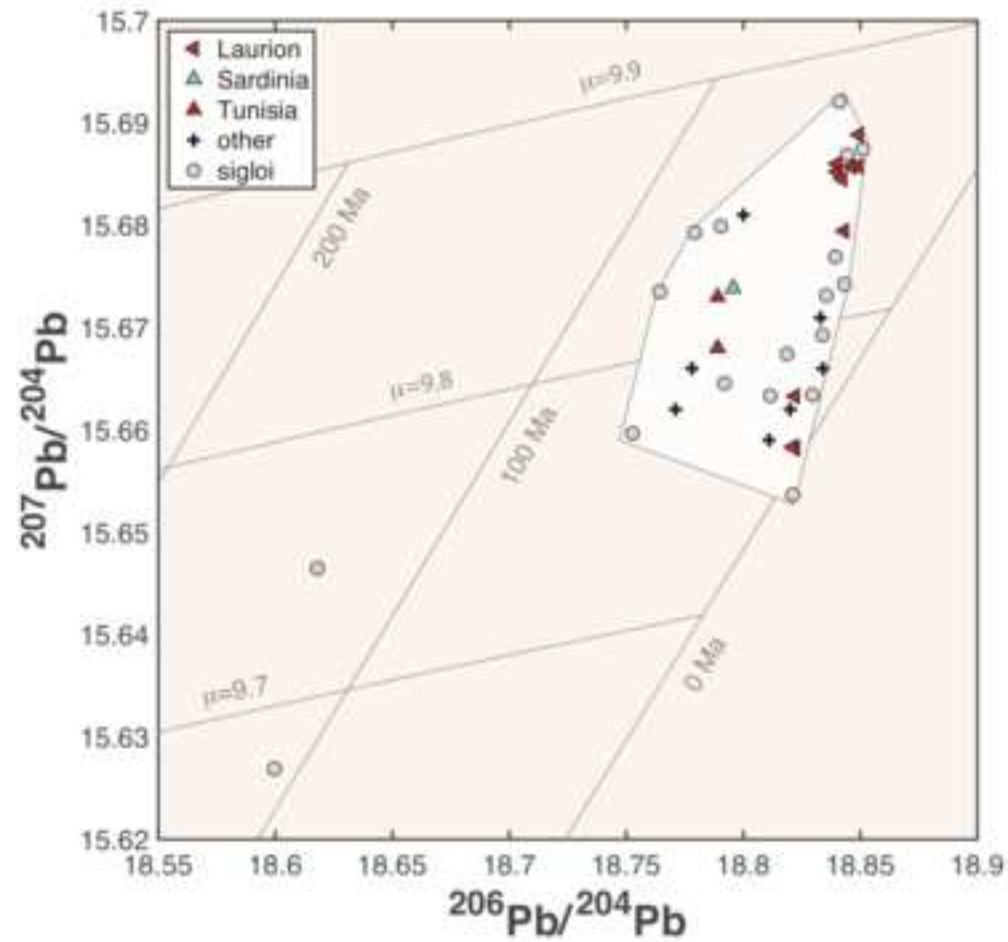
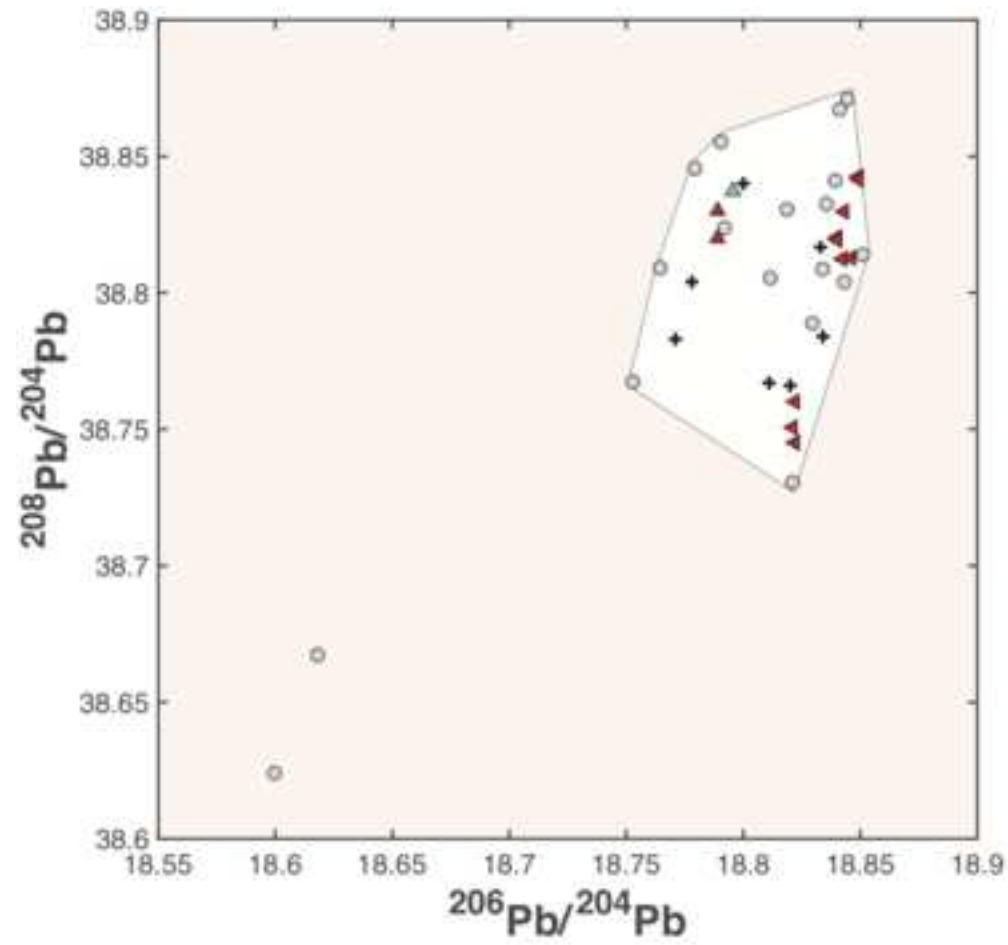


Figure 3





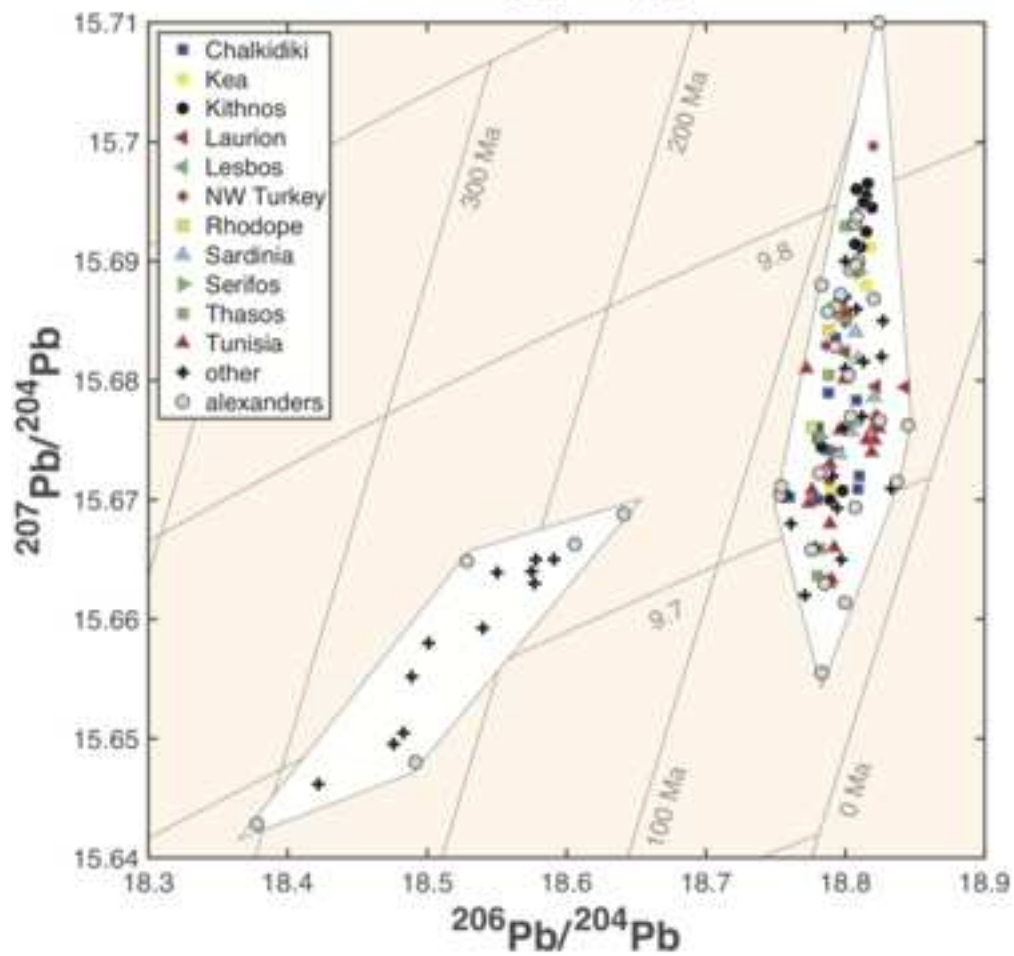
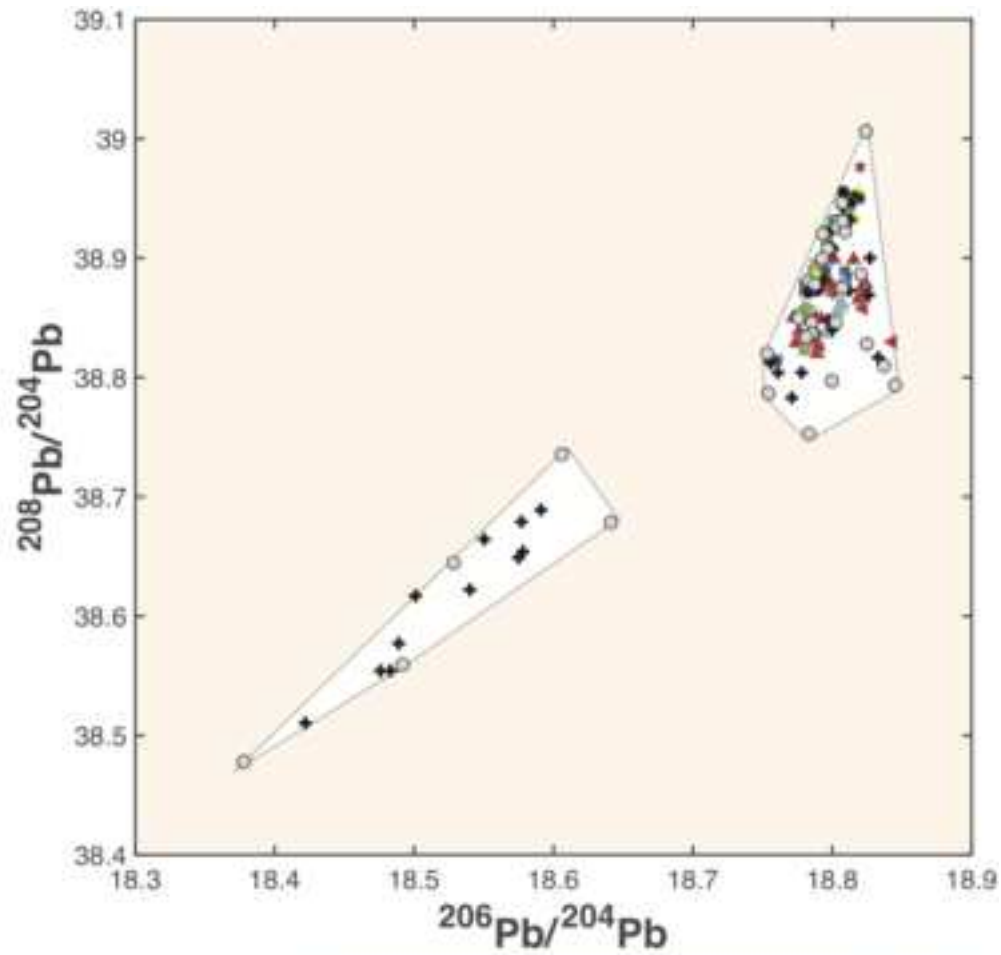
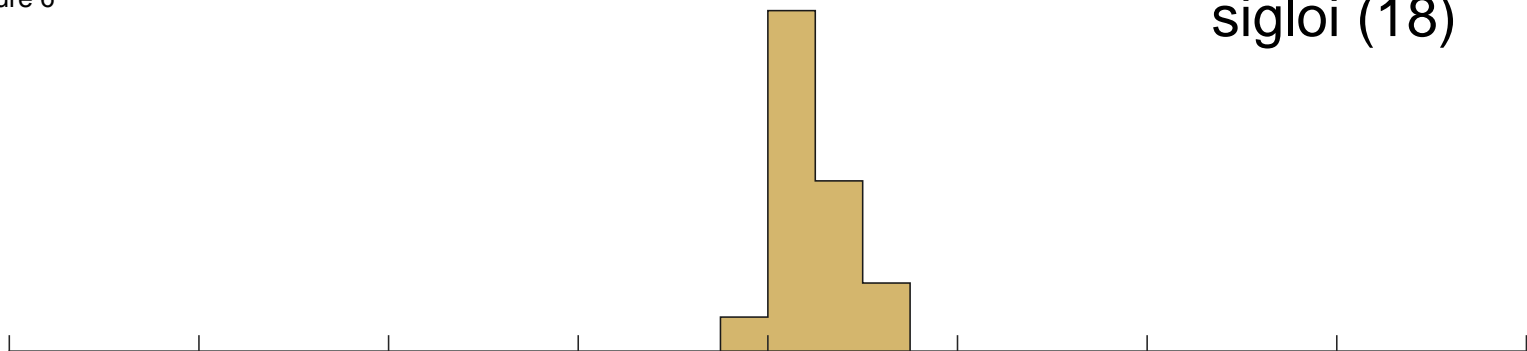
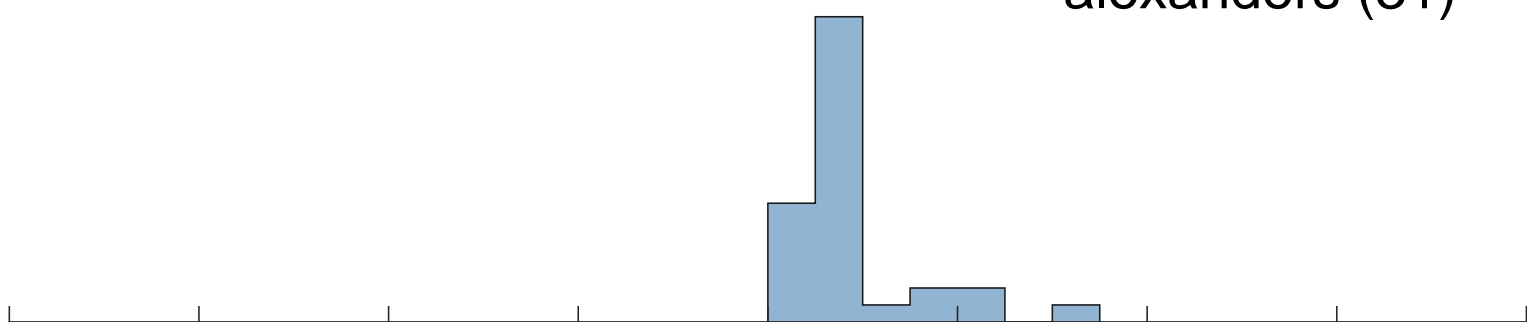


Figure 6

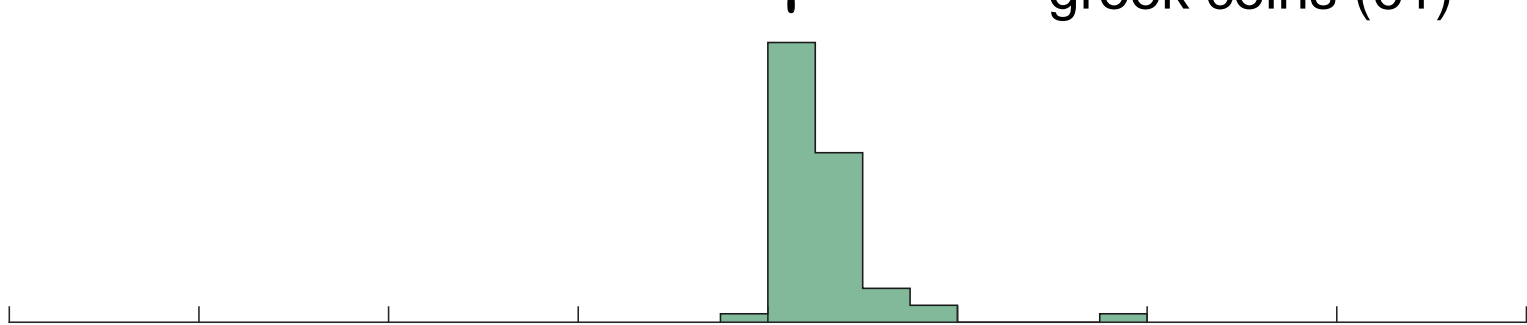
sigloi (18)



alexanders (31)



greek coins (61)



indian (36)

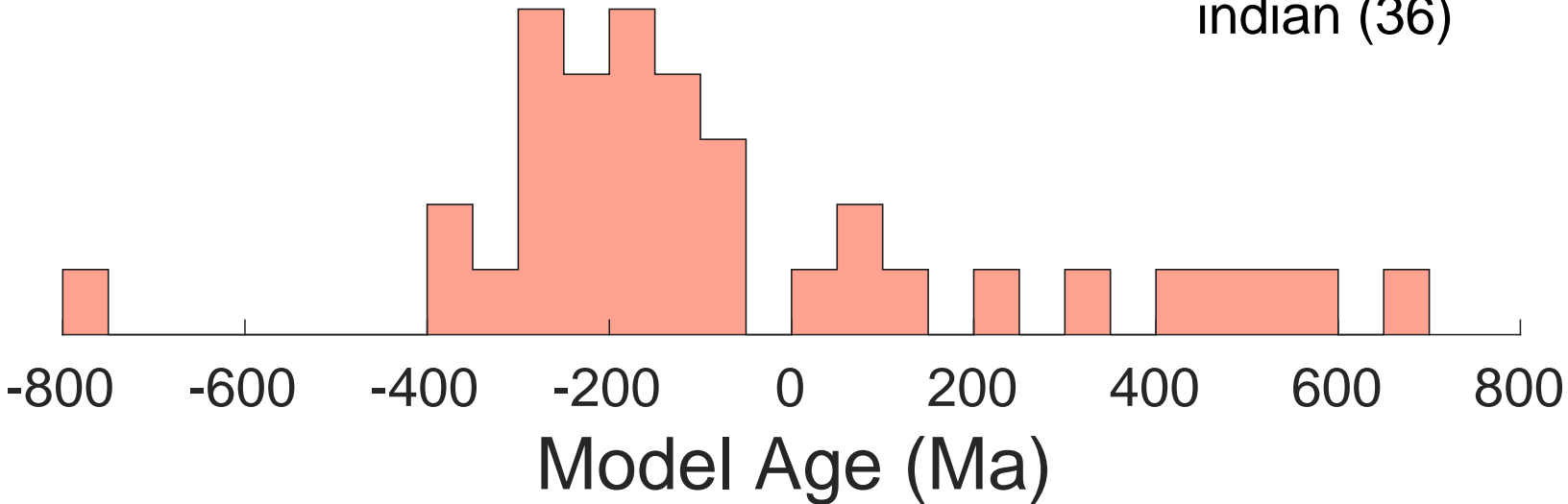


Figure 7

5Au/Ag

Cu/Ag

Pb/Ag

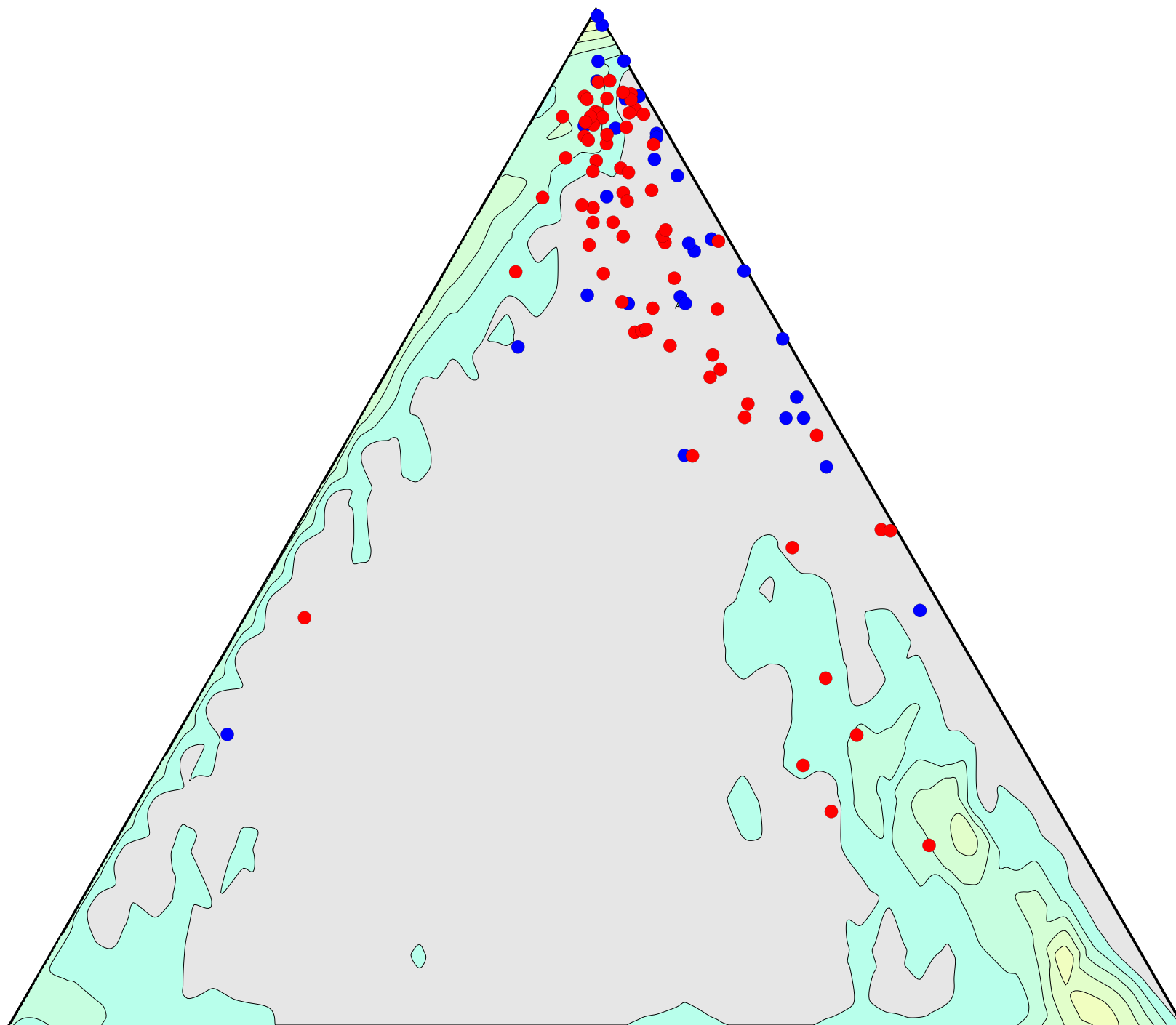


Table S1. Pb isotopic ratios and model parameters of the samples analyzed. See Milot et al. (2021) and manuscript text for average uncertainties.

Lab code #	Origin	Denomination	Origin	Inventory	Chronology	206Pb/204Pb	207Pb/204Pb	208Pb/204Pb	207Pb/206Pb	208Pb/206Pb	Tmod (Ma)	mu	kappa	code
Sigloi														
P277	Persia	siglos		Wallin Mynthandel 60130	420-375 BC	18.7644	15.6735	38.809	0.83527	2.06825	77	9.824	3.881	1
P277b	duplicate	siglos				18.7528	15.6597	38.767	0.83507	2.06731	58	9.773	3.863	1
P278	Persia	siglos	Darios I - Xerxes II	Alibaba yun 241		18.8211	15.6537	38.731	0.83171	2.05779	-6	9.738	3.799	1
P279	Persia	siglos	Darios I - Xerxes II	Alibaba yun 242		18.8445	15.6869	38.871	0.83385	2.06272	43	9.861	3.866	1
P289	Persia	siglos	Byzantium, Thrace	FORVM LT91384	387-30 BC	18.7904	15.6799	38.855	0.83447	2.06785	70	9.844	3.89	1
P296	Persia	siglos	Great King	FORVM LT 91060	c. 400 BC	18.8431	15.6742	38.804	0.83182	2.05926	19	9.812	3.829	1
P309	Persia	siglos IIIb	Lydia, Sardis, Artaxerxes I - Darius III	Rosen 673 SGCV II 4682 FORVM GA 91814	c.485-420 BC	18.8115	15.6633	38.805	0.83265	2.06287	21	9.776	3.846	1
P312	Persia	siglos IIIb	Lydia, Sardis, Artaxerxes I - Darius III	Rosen 673 SGCV II 4682 FORVM GA 91813	c. 480-420 BC	18.8393	15.6769	38.841	0.83213	2.06171	27	9.823	3.851	1
P312b	Persia	siglos IIIb	Lydia, Sardis, Artaxerxes I - Darius III	Rosen 673 SGCV II 4682 FORVM GA 91813	c. 480-420 BC	18.8355	15.6731	38.833	0.83210	2.06166	23	9.81	3.848	1
P315	Persia	siglos IIIb	Lydia, Sardis, Artaxerxes I - Darius III	Rosen 673 SGCV II 4682 FORVM GA 91816	c. 485-420 BC	18.7920	15.6645	38.824	0.83356	2.06592	38	9.785	3.868	1
P319	Caria	tetartermerion	Hekatomnos	SNG Keckman 848 SNG Kayhan 837 Klein 507 FORVM GS 89700	c. 392-277 BC	18.8186	15.6674	38.830	0.83254	2.06340	24	9.791	3.855	1
P332	Persia	1/3 siglos	Sardis Achaemenid Darius I	Lanz	552-486 BC	18.8510	15.6874	38.814	0.83218	2.05890	40	9.862	3.834	1
P409	Persia	1/4 siglos	Xerxes II - Artaxerxes II	Münzen Sänn	c. 455-420 BC	18.7793	15.6793	38.846	0.83491	2.06851	77	9.844	3.892	1
P411	Persia	siglos	Artaxerxes II	André Cichos		18.6180	15.6465	38.667	0.84041	2.07683	133	9.748	3.893	1
P412	Persia	siglos	Darius II - Artaxerxes II	G. Henzen SNG Cop 284 Klein 763 Rosen 677	420-395 BC	18.8338	15.6693	38.809	0.83197	2.06056	16	9.795	3.836	1
P413	Persia	siglos	Artaxerxes II	Ingemar Wallin Utveckling	420-375 BC	18.8411	15.6921	38.867	0.83285	2.06289	56	9.881	3.868	1
P414	Persia	1/4 siglos	Darius II - Artaxerxes II	Ingemar Wallin Utveckling	c. 404-358 BC	18.8295	15.6634	38.789	0.83185	2.05998	8	9.774	3.827	1
P415	Persia	siglos	Xerxes II - Artaxerxes II	Ingemar Wallin Utveckling	420-375 BC	18.5997	15.6269	38.624	0.84016	2.07658	108	9.676	3.876	1
Alexanders														
Alex1*	Thrace		Abydos, Alexander III	Price 1575	320-297 BC	18.7830	15.6880	38.881	0.83522	2.07001	91	9.877	3.91	2
Alex2*	Macedonia		Alexander III		336-323 BC	18.8240	15.7100	39.006	0.83457	2.07214	104	9.954	3.954	2
Alex3*	Macedonia		Alexander III	Inumis		18.8040	15.6770	38.931	0.83371	2.07036	54	9.83	3.918	2
B058	Thrace		Mesembria	Plateau 118 :	120-80 BC	18.6411	15.6688	38.678	0.84056	2.07489	159	9.83	3.892	2
B059	Macedonia		Uranopolis Lifetime Alexander II	Plateau 143 : coll. L. de Hirsch 1065	332-290 BC	18.6060	15.6663	38.736	0.84199	2.08183	180	9.828	3.943	2
B060	Macedonia		Uranopolis	Plateau 143 : Acq. 1912	332-290 BC	18.3780	15.6428	38.478	0.85117	2.09370	304	9.786	3.951	2
B061	Macedonia		Uranopolis	Plateau 143 : coll. L. de Hirsch 1067	332-290 BC	18.4917	15.6480	38.559	0.84621	2.08520	230	9.781	3.92	2
B062	Macedonia		Tarsos Lifetime Alexander III	Plateau 143 : coll. L. de Hirsch 1081	332-290 BC	18.5285	15.6649	38.645	0.84543	2.08566	235	9.839	3.946	2
P272	Macedonia	drachm	Alexander III	Andre Cichos 831/2019	336-323 BC	18.7533	15.6704	38.820	0.83559	2.07001	79	9.814	3.892	2
P286	Ionia	drachm	Colophon, Alexander III	Pasargad 25016		18.7851	15.6630	38.846	0.83244	2.06790	40	9.78	3.883	2
P287	Peloponnese	tetradrachm	Corinth, Alexander III	Artifact Man 624199	310-290 BC	18.8371	15.6715	38.810	0.83196	2.06032	18	9.803	3.835	2
P333	Macedonia	drachm	Antigonos Monophtalmus	cgb bgr_576943	310-301 BC	18.7831	15.6555	38.753	0.83349	2.06313	27	9.752	3.853	2
P335	Macedonia Alexander Philippe III	drachm	Macedonia Alexander Philippe III	cgb bgr_560215	323-317 BC	18.7929	15.6862	38.920	0.83465	2.07100	80	9.868	3.923	2
P337	Thrace	drachm	Lysimachos	cgb bgr_572924	299/298-297/296 BC	18.7759	15.6658	38.850	0.83436	2.06914	53	9.792	3.891	2
P338	Macedonia	drachm	Demerios Poliorcetes	cgb bgr_313732	291-290 BC	18.7542	15.6711	38.787	0.83560	2.06823	79	9.817	3.875	2
P339	Macedonia	drachm	Antigonos Monophtalmus	Müller 290 Price 2279 FORVM SL 79268	310-301 BC	18.7853	15.6723	38.837	0.83429	2.06743	59	9.816	3.881	2
P340	Macedonia	tetradrachm	Alexander Philippe III Arrhidaios and Alexander IV	Müller P103 Price P182 FORVM GS 87632	323-317 BC	18.8450	15.6763	38.793	0.83185	2.05849	22	9.82	3.824	2
P341	Macedonia	drachm	Antigonos I Monophtalmus	Müller 821, Price 1406 FORVM SL 21985	310-301 BC	18.8247	15.6767	38.828	0.83278	2.06262	38	9.825	3.854	2
P352	Ionia	drachm	Colophon, Alexander III	Muller 315 - Price 1762 - SNG Copenhagen 994	323-319 BC	18.7967	15.6872	38.908	0.83457	2.06988	80	9.871	3.915	2
P353	Thrace	drachm	Abydos Alexander III	Muller 1618 - Price 1528 - SNG Copenhagen 994	310-301 BC	18.8024	15.6804	38.846	0.83394	2.06604	62	9.844	3.878	2
P354	Phoenicia	tetradrachm	Byblos, Alexander III	Muller 1375 - Price 3426	330-320 BC	18.7997	15.6614	38.797	0.83307	2.06368	26	9.771	3.849	2
P355	Ionia	drachm	Colophon, Alexander III	Muller 317 - Price 1759 ; sng Copenhagen 1750	323-319 BC	18.8069	15.6932	38.946	0.83444	2.07083	84	9.892	3.93	2
P356	Ionia	drachm	Colophon, Alexander III	Muller 796 - Price 1808	310-301 BC	18.8084	15.6937	38.927	0.83440	2.06976	84	9.894	3.919	2
P357	Ionia	drachm	Colophon, Alexander III	Muller 796 - Price 1808	310-301 BC	18.8035	15.6893	38.926	0.83438	2.07012	79	9.878	3.92	2
P358	Ionia	drachm	Colophon, Alexander III	SNG Copenhagen 994	323-319 BC	18.8204	15.6869	38.887	0.83351	2.06619	61	9.865	3.889	2
P359	Ionia	drachm	Magnesia, Alexander III	Muller ; Thompson/ Bellinger, Magnesia, 5, Price 1940	323-319 BC	18.7814	15.6722	38.834	0.83445	2.06765	61	9.816	3.882	2
P360	Mysia	Drachm	Lampsakos Alexander III	Muller 531 - Price 1365	323-317 BC	18.7874	15.6858	38.878	0.83492	2.06940	84	9.867	3.905	2
P361	Egypt	drachm	Alexander III	Muller 252 ; SNG Copenhagen 972, Price 1560	310-301 BC	18.8071	15.6694	38.875	0.83317	2.06701	36	9.8	3.886	2
P362	Ionia	drachm	Colophon, Antigonos I Monophtalmus	Price 1813 ARS coins Wien g181	310-301 BC	18.8092	15.6900	38.922	0.83418	2.06928	76	9.879	3.915	2
P363	Macedonia	drachm	Alexander III Philip III	Price (1991) 2637	322-319/8 BC	18.8073	15.6897	38.931	0.83424	2.06997	77	9.878	3.921	2
P364	Macedonia	drachm	Alexander III Philip III	Sear (1979) 6750	323-317 BC	18.7928	15.6829	38.900	0.83449	2.06994	74	9.855	3.912	2
Greek silver coinage														
P271	Thrace		Apollonia Pontika	Andre Cichos 831/2019	450-440 BC	18.7788	15.6436	38.747	0.83304	2.06334	6	9.707	3.83	3
P273	Thrace	hemidrachm	Chersonesos, Lion	K. B coins 1471	386-338 BC	18.8416	15.6831	38.826	0.83236	2.06059	38	9.847	3.844	3
P274	Thrace	hemidrachm	Chersonesos, Lion	K. B coins 1471	386-338 BC	18.7752	15.6550	38.806	0.83380	2.06687	32	9.751	3.866	3
P275	Caria	Obol	Miletos	Blitz 123853797239	600-500 BC	18.8037	15.6596	38.877	0.83278	2.06749	19	9.764	3.885	3
P276	Thrace	Obol	Abdera	Blitz 123853803035	475-450 BC	18.8259	15.6736	38.830	0.83257	2.06255	31	9.813	3.853	3
P280	Thrace	Hemidrachme	Chersonese	Inumis MC/16/03780		18.7925	15.6742	38.839	0.83407	2.06674	57	9.821	3.879	3
P281	Caria	Obol	Miletos	Inumis MC/15/00572	C500 BC	18.8544	15.6853	38.837	0.83192	2.05983	33	9.853	3.842	3
P282	Mysia	Obol	Kysikos	Inumis MC/17/05961		18.8038	15.6774	38.822	0.83372	2.06455	55	9.832	3.864	3
P283	Mysia	Obol	Kysikos	Numismatik Lanz 303205463793 NER 122		18.7910	15.6529	38.843	0.83300	2.06702	15	9.74	3.874	3

P284	Ionia	Hemidrachme	Magnesia	Numismatik Lanz 372698845567 NER 125		18.7908	15.6588	38.823	0.83332	2.06608	28	9.763	3.866	3
P285	Macedonia	Tertobol	Terone	Numismatik Lanz 303213684949 CCT469		18.7886	15.6383	38.816	0.83234	2.06593	-12	9.685	3.856	3
P288	Lesbos	Diobol	Mytilene	FORVM LT91384 BMC 8	400-350 BC	18.8257	15.6742	38.832	0.83259	2.06270	32	9.815	3.854	3
P290	Thrace	Hemidrachm	Chersonese	FORVM LT91384	386-338 BC	18.7347	15.6541	38.773	0.83558	2.06952	60	9.755	3.875	3
P291	Thessaly	Hemidrachm	Magnesia	FORVM LT91384	350-325 BC	18.7738	15.6586	38.764	0.83406	2.06486	40	9.765	3.848	3
P292	Lycia	Hemidrachm	Lycian league	FORVM LT91384	167-88 BC	18.6194	15.6519	38.769	0.84063	2.08218	142	9.769	3.946	3
P293	Mysia	Hemiobol	Cyzicus	FORVM LT91384	450-400 BC	18.7477	15.6733	38.820	0.83598	2.07062	89	9.827	3.897	3
P294	Thrace	Hemidrachm	Abydos	FORVM LT91384	350-325 BC	18.8183	15.6839	38.867	0.83344	2.06539	57	9.854	3.88	3
P297	Cyzicus	drachm	Cyzicus	FORVM LT 91060	390-341 BC	18.8324	15.6840	38.855	0.83281	2.06321	47	9.852	3.865	3
P299	Ionia	hemiobol	Ionia	FORVM LT 91060 uncertain		18.8373	15.6812	38.816	0.83245	2.06052	37	9.84	3.841	3
P300	Tenedos	Obol	Tenedos	FORVM LT 91060 SNG Cop 509	450-387 BC	18.8350	15.6815	38.833	0.83256	2.06169	40	9.842	3.851	3
P301	Mysia	Obol	Cyzicus	FORVM LT 91060		18.7469	15.6735	38.867	0.83606	2.07323	90	9.828	3.921	3
P302	Caria	1/48th Stater	Miletos	FORVM LT 91060		18.8457	15.6782	38.830	0.83193	2.06043	25	9.827	3.842	3
P303	Bruthium Rhegion	Obol	Bruthium Rhegion	FORVM LT 91060 Klein 430	c.510 BC	18.7882	15.6498	38.842	0.83296	2.06738	11	9.729	3.874	3
P304	Sicily, Panormos	Obol	Panormos	FORVM LT 91060		18.7633	15.6722	38.807	0.83526	2.06826	75	9.82	3.88	3
P305	Sicily	litra	Sicily, segesta	FORVM LT 91060		18.8105	15.6609	38.765	0.83257	2.06079	17	9.767	3.826	3
P306	Lycia	obol	Lycia	FORVM LT 91060	440-410 BC	18.7964	15.6741	38.793	0.83388	2.06379	54	9.82	3.853	3
P307	Thrace	hemidrachm	Chersonesos	McClean II 4076 SNG Cop 843 HGC 3 1437 FORVM GS 91079	c.400-338 BC	18.8233	15.6717	38.840	0.83257	2.06342	29	9.806	3.859	3
P308	Thrace	hemidrachm	Chersonesos	McClean II 4102 Weber II 2421 SNG Cop 836 FORVM GS 91078	c.400-338 BC	18.8212	15.6640	38.796	0.83227	2.06129	15	9.777	3.825	3
P310	Thasos	hemiobol	Thasos	Le Rider 12 SNG Cop 1033 Fitzwilliam 3665 McClean 42218 FORVM GS 89783	c.411-404 BC	18.6088	15.6452	38.726	0.84074	2.08104	137	9.745	3.939	3
P311	Caria	1/12 stater	Miletos	SNG Kayhan 476 SNG Cop944 SGCV II 3532 FORVM GA91987	late 6th century BC	18.7974	15.6526	38.862	0.83271	2.06748	10	9.738	3.879	3
P313	Peloponnese	Triobol	Argos Argolis	BCD Pelopon 1023 HGC 5 663 FORVM GS 91476	c.480-430 BC	18.8439	15.6778	38.838	0.83198	2.06101	26	9.826	3.847	3
P314	Thrace	hemidrachm	Chersonesos	SNG Cop 834 FORVM GS 91352	c.400-338 BC	18.8385	15.6792	38.840	0.83230	2.06171	33	9.832	3.852	3
P316	Thasos	trihebiobol	Thasos	Le Rider 27 SNG Cop 1029 Dewing 1331 SGCV 1755 FORVM GS 89789	c.404-355 BC	18.7874	15.6696	38.874	0.83406	2.06917	52	9.805	3.897	3
P317	Thasos	diobol	Thasos	Le Rider 4 HGC 6 333 Rosen 144 SNG Cop 191 FORVM GS 89782	c.525-480 BC	18.8478	15.6693	38.960	0.83293	2.06715	6	9.793	3.902	3
P318	Thrace	Hemidrachm	Chersonesos	Weber II 2420 McClean 4113 HGC 3 1437 FORVM GS 91076	c.400-338 BC	18.7883	15.6586	38.855	0.83341	2.06805	29	9.762	3.884	3
P320	Thrace	hemidrachm	Chersonesos	McLean II 4079 SNG Ashm 3589 Weber 2419 FORVM GS 91071	c.400-338 BC	18.8163	15.6628	38.798	0.83242	2.06199	16	9.773	3.839	3
P320b	Thrace duplicate	hemidrachm	Chersonesos	McLean II 4079 SNG Ashm 3589 Weber 2419 FORVM GS 91071	c.400-338 BC	18.8291	15.6740	38.819	0.83243	2.06159	29	9.814	3.845	3
P321	Mysia	obol	dolphin, Cyzicus	von Fritze I FORVM GS 91171	525-475 BC	18.7939	15.6656	38.890	0.83355	2.06927	39	9.788	3.9	3
P322	Mysia	trihebiobol (hemihek)	Phokaia	SNG Kayhan 525 von Aulock 1813 FORVM GA88960 823	c.500 BC	18.6235	15.6554	38.680	0.84062	2.07689	146	9.782	3.899	3
P323	Thrace	Hemiobol	Pantikapsion	SNG Fitzwilliam 1592 Klein 73 McClean 4442 FORVM GA86537 309	480-470 BC	18.8388	15.6769	38.837	0.83217	2.06159	28	9.823	3.85	3
P324	Mysia	Hemiobol	Cyzicus	SNG BNF 359 FORVM GA91752 722	600-550 BC	18.4062	15.5973	38.418	0.84739	2.08728	196	9.6	3.884	3
P325	Peloponnese	Diobol	Korinth	BCD 36 Kölner Münzkabinett 21561	500-450 BC	18.8091	15.6661	38.795	0.83290	2.06259	28	9.788	3.843	3
P326	Mysia	Obol	Cyzicus	Von Fritze II 15SNG BN 380-4 Romae Aeternae Numismatics	450-400 BC	18.7782	15.6725	38.811	0.83462	2.06683	64	9.818	3.873	3
P327	Aegina	Obol	Aegina	SNG Cop 505 Romae Aeternae Numismatics	18.6983	15.6575	38.805	0.83737	2.07529	94	9.775	3.915	3	
P328	Ionia	Drachm	Colophon, Alexander Philippe Arrhidaios	Price P46 Ars Coin g192	322-319 BC	18.8257	15.6946	38.949	0.83368	2.06898	73	9.894	3.92	3
P329	Mysia	Diobol	Cyzicus	BMC 15-34 Ars Coin g218	480-400 BC	18.7814	15.6725	38.873	0.83450	2.06976	62	9.817	3.902	3
P329b	Mysia	Obol	Cyzicus	Ars Coin g218	480-400 BC	18.7623	15.6550	38.813	0.83439	2.06867	41	9.753	3.878	3
P330	Mysia	Stater	Cyzicus	Von Fritze II 15 SNG Fr 380-384 Ars Coin g40	480 BC	18.8502	15.6828	38.857	0.83197	2.06136	31	9.844	3.854	3
P331	Peloponnese	stater	Corinth	cgb bgr_556764	340 BC	18.8440	15.6783	38.820	0.83200	2.06007	27	9.828	3.838	3
P336	Euboea	tetrobol	Histiaea	cgb bgr_594611	196-168 BC	18.5727	15.6420	38.679	0.84221	2.08259	158	9.74	3.927	3
Dr*	Istros	drachm	Istros		500-300 BC	18.772	15.684	38.876	0.8355	2.0710	92	9.863	3.913	3
Ob1*	Istros	obol	Istros		500-300 BC	18.767	15.684	38.897	0.8357	2.0726	95	9.864	3.927	3
Ob2*	Istros	obol	Istros		500-300 BC	18.823	15.694	38.931	0.8338	2.0683	73	9.892	3.912	3
Ob3*	Istros	obol	Istros		500-400 BC	18.861	15.699	38.897	0.8324	2.0623	55	9.904	3.873	3
pont1*	Thrace	drachm	Apollonia Pontika		500-400 BC	18.852	15.697	38.894	0.8326	2.0631	58	9.898	3.877	3
Pont2*	Thrace	drachm	Apollonia Pontika		500-400 BC	18.711	15.685	38.916	0.8383	2.0798	139	9.879	3.973	3
Pont3*	Thrace	drachm	Apollonia Pontika		500-400 BC	18.821	15.681	38.965	0.8332	2.0703	49	9.842	3.926	3
Gr1*	Attica	drachm	Athens	Hafnia Coins Sear 2537	393-300 BC	18.858	15.701	38.914	0.8326	2.0635	61	9.912	3.884	3
Gr2*	Caria	diobol	Miletos	Hafnia Coins Sear 3532	c.500 BC	18.274	15.645	38.436	0.8561	2.1033	385	9.820	4.000	3
Gr3*	Pharsalos	hemidrachm	Pharsalos	Sear 2189	450-400 BC	18.842	15.695	38.900	0.8330	2.0645	61	9.892	3.885	3
ph1*	Phoenicia	1/8 shekel	Sidon	Sear 5940	333 BC	18.920	15.696	39.178	0.8296	2.0707	5	9.882	3.973	3
Indian kingdoms														
P334	India	shana	Gandhara	cgb bgr_587090	500-331 BC	19.0865	15.7154	39.639	0.82339	2.07681	-79	9.928	4.097	4
P374	India	karshapana	Magadha, GH 233		550-461 BC	18.0430	15.7045	37.907	0.87039	2.10094	657	10.133	3.883	4
P375	India	drachm	Annuruddha-Nagadasaka period, Magadha GH 320		445-413 BC	18.3919	15.7436	38.346	0.85600	2.08492	477	10.188	3.905	4
P376	India	1/8 shatamana	Gandhara Janapada		c.500-400 BC	19.2560	15.7171	39.900	0.81622	2.07211	-203	9.908	4.112	4
P377	India	shatamana	Gandhara		c.600-500 BC	19.1184	15.7077	39.554	0.82161	2.06899	-119	9.893	4.003	4
P378	India	shatamana	Gandhara		c.500-400 BC	18.6164	15.7440	38.813	0.84569	2.08486	318	10.132	4.034	4
P379	India	shatamana	Gandhara		c.500-400 BC	19.4476	15.7343	40.321	0.80905	2.07332	-311	9.945	4.189	4
P380	India	shatamana	Gandhara		c.600-500 BC	18.8316	15.6673	38.837	0.83197	2.06234	14	9.788	3.851	4
P381	India	drachm	Magadha, Bhattiya to Ajatashatru		c.550-461 BC	18.3497	15.7507	38.167	0.85836	2.07995	519	10.229	3.838	4
P382	India	karshapana	Mauryan Empire			19.2707	15.7302	40.191	0.81627	2.08561	-187	9.954	4.242	4

P383	India	karshapana	Mauryan Empire		19.1485	15.7473	40.055	0.82239	2.09187	-61	10.038	4.266	4
P384	India	karshapana	Gandhara	c. 600-500 BC	19.3305	15.7191	40.147	0.81315	2.07671	-255	9.905	4.179	4
P385	India	karshapana	Panchala		18.3715	15.7955	38.026	0.85979	2.06988	580	10.408	3.762	4
P386	India	karshapana	Panchala		20.8712	16.0174	38.516	0.76744	1.84541	-752	10.818	2.829	4
P387	India	karshapana	Gandhara	c. 600-500 BC	19.6064	15.7533	40.738	0.80348	2.07781	-390	9.995	4.282	4
P388	India	shatamana	shatamana	c. 600-500 BC	19.2451	15.7771	40.126	0.81980	2.08497	-73	10.135	4.247	4
P389	India	Early 1/2 shatamana	Early 1/2 shatamana	c. 600-500 BC	19.2336	15.7312	40.145	0.81789	2.08721	-157	9.964	4.246	4
P390	India	Early 1/2 shatamana	Early 1/2 shatamana	c. 600-500 BC	19.3170	15.7389	40.172	0.81474	2.07961	-203	9.98	4.207	4
P391	India	Early 1/2 shatamana	Early 1/2 shatamana	c. 600-500 BC	18.6179	15.6824	38.701	0.84230	2.07861	202	9.888	3.923	4
P392	India	Early 1/2 shatamana	Early 1/2 shatamana	c. 600-500 BC	19.1935	15.7298	40.051	0.81952	2.08667	-130	9.965	4.228	4
P393	India	Early 1/2 shatamana	Early 1/2 shatamana	c. 600-500 BC	19.5297	15.7382	40.565	0.80585	2.07708	-365	9.949	4.248	4
P394	India	Early 1/2 shatamana	Early 1/2 shatamana	c. 600-500 BC	18.6294	15.6515	38.665	0.84014	2.07542	134	9.765	3.887	4
P395	India	Early 1/8 shatamana	Early 1/8 shatamana	c. 600-500 BC	19.1291	15.7137	39.940	0.82145	2.08788	-115	9.914	4.211	4
P396	India	Early 1/8 shatamana	Early 1/8 shatamana	c. 600-500 BC	19.3201	15.7285	40.307	0.81406	2.08622	-227	9.941	4.263	4
P397	India	Early 1/8 shatamana	Early 1/8 shatamana	c. 600-500 BC	19.4086	15.7424	40.317	0.81111	2.07719	-265	9.98	4.215	4
P398	India	Early 1/8 shatamana	Early 1/8 shatamana	c. 600-500 BC	18.7748	15.6822	39.110	0.83529	2.08316	86	9.856	4.028	4
P399	India	Early 1/8 shatamana	Early 1/8 shatamana	c. 600-500 BC	19.1751	15.7046	39.906	0.81900	2.08109	-168	9.873	4.161	4
P400	India	Early 1/8 shatamana	Early 1/8 shatamana	c. 600-500 BC	19.1938	15.7184	40.077	0.81891	2.08800	-153	9.922	4.235	4
P401	India	1/4 shatamana	Latest types or different denomination 1/4 shatamana ??		19.0908	15.6871	39.505	0.82172	2.06928	-141	9.82	4.019	4
P402	India	1/4 shatamana	Latest types or different denomination 1/4 shatamana ??		19.2942	15.7350	40.276	0.81551	2.08746	-194	9.969	4.268	4
P403	India	1/4 shatamana	Latest types or different denomination 1/4 shatamana ??		19.4350	15.7408	40.335	0.80993	2.07542	-288	9.971	4.206	4
P404	India	1/4 shatamana	Latest types or different denomination 1/4 shatamana ??		18.2925	15.6645	38.468	0.85632	2.10297	407	9.894	4.011	4
P405	India	1/4 shatamana	Latest types or different denomination 1/4 shatamana ??		18.9035	15.7160	39.448	0.83138	2.08686	57	9.962	4.124	4
P406	India	1/4 shatamana	Latest types or different denomination 1/4 shatamana ??		19.2969	15.7251	40.084	0.81489	2.07718	-217	9.932	4.173	4
P407	India	karshapana	Mauryan Empire		19.4102	15.7384	40.317	0.81082	2.07702	-274	9.965	4.213	4
P408	India	karshapana	Mauryan Empire		19.4185	15.7449	40.304	0.81082	2.07567	-267	9.988	4.204	4

* Data from Desautly et al. (2011)